

# Geochemistry of Siliciclastic Rocks from the Koira Group of Western Iron Ore Group, Singhbhum Craton, Eastern India: Implications for Provenance, Paleo-Weathering, and Tectonic Setting

Pawan Kumar Yadav<sup>1</sup>, Manorama Das<sup>2</sup>

Geological Survey of India, SU: Bihar, Lohiya Nagar, Kankarbagh, Patna – 800020, India

\*Corresponding author's email: [pawankumaryadavgsi\[at\]gmail.com](mailto:pawankumaryadavgsi[at]gmail.com)

**Abstract:** *The geochemical characteristics of quartz-pebble conglomerate (QPC) and quartzite from the Koira Group of western Iron Ore Group, Singhbhum Craton, eastern India have been studied in the context of provenance, paleoweathering, and tectonic setting. In the binary plots of  $\log(\text{SiO}_2/\text{Al}_2\text{O}_3)$  vs.  $\log(\text{Na}_2\text{O}/\text{K}_2\text{O})$  and  $\log(\text{SiO}_2/\text{Al}_2\text{O}_3)$  vs.  $\log(\text{Fe}_2\text{O}_3/\text{K}_2\text{O})$ , QPC samples occupy the fields of arkose, sub-arkose, sub-litharenite, and quartz-arenite, and quartzites fall in sub-arkose to sub-litharenite fields. In bivariate diagrams of  $\text{TiO}_2$  vs. Zr and DF-1 vs. DF-2 respectively were used for depicting the provenance of these sequences, and all the samples of QPC and quartzite fall in the felsic igneous rocks and granites and gneisses field respectively. Besides, the values of Pb, U, Th, Y, La, Ce, and low Sc with high critical trace elemental ratios of Th/U, Th/Sc, Zr/Y, and La/Sc in QPC indicating their derivation from the felsic igneous source. In contrast, both felsic and mafic sources are responsible for the formation of quartzites which are supported by the presence of a low concentration of Th and Sc and variable ratios of Th/Sc. Eu anomaly in QPC and quartzite varies from 0.32 to 0.67 and 0.29 - 1.63 respectively which is attributed to the presence of Eu depleted felsic igneous rocks in the provenance such as granites. Based on the Chemical Index of Alteration (CIA) values, a high degree of chemical weathering was depicted in the sequence of QPC and quartzite. In the A-CN-K diagram, the majority samples fall between the granodiorite and tonalite fields which indicate the probable source for the QPC-quartzite sequence. The value of the Plagioclase Index of Alteration (PIA), all the samples falls between oligoclase (Olg) and albite (Ab) fields of the AK-C-N ternary diagram which indicates that the plagioclase was completely altered. In  $\text{Al}_2\text{O}_3/\text{SiO}_2$  vs.  $\text{Fe}_2\text{O}_3+\text{MgO}$ ,  $\text{TiO}_2$  vs.  $\text{Fe}_2\text{O}_3+\text{MgO}$ , and  $\text{SiO}_2$  vs.  $\text{K}_2\text{O}/\text{Na}_2\text{O}$  diagrams, all the samples of QPC and quartzites dominantly come in the field of passive margin tectonic setting except few samples fall in the active continental margin and continental arc fields respectively. Based on the above observations, it can be inferred that the QPC and quartzite were predominantly deposited in a passive margin tectonic setting developed during the Archean along the western margin of Singhbhum Craton.*

**Keywords:** Quartz-pebble conglomerate-Quartzite sequence, Provenance, Paleo-weathering, Tectonic setting, Singhbhum Craton, Eastern India

## 1. Introduction

Quartz-pebble conglomerates (QPCs) are known for hosting of uranium, gold, and REE deposits which were deposited in a fluvial system over a cratonised granite-greenstone basement. QPCs are mainly restricted to the Neoproterozoic and Paleoproterozoic and do not occur in sediments younger than about 2200 Ma. QPCs are predominantly reported from Huronian Supergroup, Elliot Lake, Woodburn Lake of Canada, Witwatersrand Supergroup in South Africa, Goias Velho in Brazil, Precambrian Dharwar Craton, and Singhbhum Craton (Robertson, 1962; Roscoe, 1973; Rama Rao, 1974; Schildowski, 1975; Theis, 1979; Grandstaff, 1980; Smith and Minter, 1980; Robinson and Spooner, 1982; Mossman and Harron, 1983; Saager and Stupp, 1983; Mahadevan, 1986; Viswanath et al., 1988; Fareeduddin, 1990; Scarpelli, 1991; Phillips and Law, 2000; Frimmel and Minter, 2002; Pandit, 2002; Yang and Holland, 2002; Bekker et al., 2004; Mikhailov, 2006; Hazen et al., 2009; Cuney, 2010; Dankert and Hein, 2010; Chakrabarti et al., 2011, 2013; Kumar et al., 2009, 2011a,b, 2012, 2017; Bergen and Fayek, 2012; Yadav and Ghosh, 2013; Uvarova et al., 2014; Ronald,

2015; Mukhopadhyay et al., 2016; Yadav et al., 2016; Yadav, 2017; Yadav and Das, 2018, 2019). In India, radioactive mineralization in QPCs are largely reported from the Precambrian Dharwar Craton and Singhbhum Craton (Vasudeva Rao et al., 1988; Das et al., 1988; Haque and Dutta, 1996, 1999, 2001; Sunilkumar et al., 1996, 1998; Mishra et al., 1997; Pandit, 2002; Mishra et al., 2008; Kumar et al., 2009, 2011a,b, 2012, 2017; Chakrabarti et al., 2011, 2013; Yadav and Ghosh, 2013; Mukhopadhyay et al., 2016; Yadav et al., 2016; Yadav, 2017; Yadav and Das, 2018, 2019).

Mukhopadhyay et al. (2016) reconstructed the provenance, tectonic setting, and paleo weathering conditions of the quartzite-conglomerate succession from the southern part of the Singhbhum Craton. The Mahagiri Quartzite, dated 3.02 Ga for their youngest detrital zircon population, is developed unconformably over the Mesoarchean Singhbhum Granite (3.44 to 3.1 Ga). The lower part mainly comprises conglomerate-pebbly sandstone sequences and the upper part consists of mature quartz arenite. The uraninite grains are recovered from quartzite, showing thorium (Th) values more than 4 wt. %, sulphur (S), and elevated concentration of REE-

Y confirmed by EPMA and SEM-EDS studies (Mukhopadhyay et al., 2016). Ghosh et al. (2016) determined the provenance, tectonic setting, and weathering characteristics of weakly metamorphosed WIOG, Singhbhum craton, eastern India based on petrographic and geochemical compositions. Detrital zircon recovered from the Keonjhar Quartzite, yielded 3.01 Ga which unconformably overlies the Singhbhum Granite (3.1 - 3.4 Ga). The high CIA values suggest a stable tectonic setting that caused the erosion rates to decrease, which in turn caused a rise in the flux of weathered materials. Granodioritic and mafic rocks might be the probable source that contributes to the formation of Keonjhar Quartzite, confirmed by the A-CN-K plot. Kumar et al. (2017) have also discussed the provenance, paleo-weathering, and tectonic setting of the QPC-quartzite sequence at the western fringe of the western Iron Ore Group and the Bonai Granite. Moderate to high chemical weathering conditions in the provenance areas of QPC and quartzites were depicted by the geochemical data like CIA, PIA, and various binary diagrams. Felsic to partly mafic-ultramafic sources for the deposition of radioactive quartz-pebble conglomerates and quartzite were attributed by the major, trace and REE data.

In this paper, provenance characterization, paleo-weathering conditions, and possible tectonic setting of the sequence of the quartz-pebble conglomerate and quartzite sequences at the eastern fringe of the western Iron Ore Group and the Singhbhum Granite have been discussed for the first time in detailed.

### Regional Geological setting and geology of the study area

The study area forms a part of the eastern segment of the Indian Precambrian shield which constitutes one of India's older records of Paleoproterozoic crust known as the Singhbhum North Orissa Craton or simply the Singhbhum Craton (Fig. 1b). The Singhbhum Craton (SC) is located within a tectonic framework of the Chottanagpur gneissic complex (CGC) in the north, the Eastern Ghats Mobile Belt (EGMB) in the south and the Baster cratonic block in the west. The rocks of Older Metamorphic Group (OMG), Older Metamorphic Tonalite Gneiss (OMTG), and Iron Ore Group (IOG) are noticed in the Singhbhum Craton (Saha, 1994). The OMG predominantly comprises pelitic schist, arenite, para, and ortho- amphibolites which are dated ~3.5 - 3.6 Ga (Saha, 1994; Misra et al., 1999; Mukhopadhyay, 2001; Misra, 2006). Tonalite-Trondhjemite-Granodiorite (TTG) suite of rocks which are known as the Older Metamorphic Tonalite Gneiss which is intruded by the rocks of the OMG. OMTG represents the early vestigial stable continental crust which is dated at 3.44 Ga by Goswami et al., 1995. The Palaeo-Mesoarchean sedimentation in the Singhbhum Craton began with the deposition of the IOG rocks which is represented by low-grade volcano-sedimentary successions comprising meta-volcanics, felsic and intermediate volcanics (Yadav and Das, 2019; Yadav et al., 2020), ultramafics, spinifex textured peridotitic komatiite (Yadav et al., 2015, 2016; Chaudhuri et al., 2015, 2017; Yadav and Das, 2017), quartz-pebble conglomerate (Yadav et al., 2016; Yadav, 2017; Yadav and Das, 2019) quartzites, banded iron formation, metachert with minor carbonate rocks

(Saha, 1994; Bhattacharya and Mahapatra, 2007; Mukhopadhyay et al., 2008, 2014). The greenstone successions of the IOG occur in three detached synformal outcrop belts, namely, the Eastern (Gorumahisani-Badampahar greenstone belt or EIOG), Western (Noamundi-Jamda-Koira greenstone belt or WIOG), and Southern (Tomka-Daitari greenstone belt or SIOG) which is exposed on the eastern, western, and southern periphery of the Singhbhum Granite pluton (Saha 1994; Fig. 1b). The Bonai-Kendujhar belt (BKB) is exposed in the form of a 'Horse Shoe' shaped syncline belonging to the WIOG (Jones, 1934, Dunn and Dey, 1942). The lithostratigraphy of WIOG is classified under the Koira Group which is mainly constituted of basal sandstone-quartzite, mafic volcanic formation, lower shale formation, banded iron formation including massive, laminated, shaly, powdery and flaky ores, upper shale formation and Kolhan Group (Murthy and Acharya, 1975). The entire area is folded into a series of asymmetrical/slightly overturned anticlines and synclines. The field contact relationship between Singhbhum Granite Phase - B and Bonai Granite in respect of the Koira Group has been proposed by several workers viz., Murthy and Acharya, 1975; Sarangi and Acharya, 1975; Saha, 1994; Mukhopadhyay, 2001; Mukhopadhyay et al., 2008, 2016; Basu et al., 2008. The rocks of BKB are flanked by Dangoaposi lavas, Nuakot volcanics and Malangtoli lavas (Dunn, 1940; Banerjee, 1982; Iyengar and Murthy, 1982; Sahu et al., 1998; Saha, 1994; Rajanikanta et al., 2017).

The study area consists of lithoassemblages of Badampahar Group comprising amphibolite and quartz-biotite schist which occurs in the western part of the area and shows the grade of metamorphism from greenschist to lower amphibolite facies. The Koira Group of rocks is represented by a quartz-pebble conglomerate (QPC), quartzite and basalt. Three varieties of Singhbhum Granitoids viz., tonalite gneiss, granodiorite/pyrophyllite schist, and porphyritic granite are mapped on the basis of field relation, mineral assemblages, and texture. The granitoids of the studied area exhibits an intrusive relationship with the Badampahar Group of rocks and forming the basement for the Koira Group of rocks. Besides, younger intrusives like dolerite and gabbro dykes are also mapped in the study area (Fig. 1c; Yadav et al., 2016; Yadav and Das, 2019). The central and eastern segments are predominantly occupied by Singhbhum Granitoids. Tonalite gneiss occurs as xenoliths within the granodiorite country rock which is observed to the west of Padmapur and south of Mahadeijora (Fig. 1c). It shows alternating felsic bands consisting of quartz, plagioclase, and K-feldspar and mafic bands with biotite, muscovite, and epidote having a thickness of the order of few millimeters to centimeters (Fig. 2a). The gneisses have been traversed by several pegmatites, and quartz veins (Fig. 2a) of different generations from pre to post deformational stage. The mapped area mostly occupied by granodiorite country rock which is leucocratic, medium to coarse-grained, massive to highly jointed and essentially composed of quartz, plagioclase, and K-feldspar with biotite and muscovite as ferromagnesian and epidote as accessories. The last variety of granite is porphyritic granite which occurs as small outcrop within the granodiorite to the west and north of Raisuan and

north of Sanker (Fig. 1c). The K-feldspar phenocrysts range from 1 to 7 cm (Fig. 2b). On the basis of the presence of granodiorite xenolith within porphyritic granite, it is inferred that the granodiorite was latterly intruded by the porphyritic granite.

The Koira Group of rocks are exposed in the western part of the study area which is represented by a quartz-pebble conglomerate (QPC), quartzite, and basalt (Fig. 1c). Seven small bands of QPC are mapped to the southeast of Bhalupahari and west of Patna area, Kendujhar district, Odisha and are interbedded with the quartzite (Fig. 1c). However, these are commonly restricted to the lower part of the sedimentary package. The clasts of conglomerate vary from pebble to granule in size which is generally framework supported with the clast/matrix ratio varying from 70:30 to 60:40 (Fig. 2c & 2d). However, in some cases, it is matrix-supported with having clast/matrix ratio of 30:70. Ninety percent of the clasts are dominantly made up of white and

smoky quartz which is mainly rounded, subrounded, and elliptical (Fig. 2c & 2d). The dimensions of these QPC bands are as follows:- (i) 400 m X 40 - 80 m extending N - S, (ii) 100 m X 20 m extending N40°E - S40°W, (iii) 150 m X 40 m extending N40°W - S40°E, (iv) 100 m X 20 m extending N60°E - S60°W, (v) 150 m X 40 m extending N45°W - S45°E, (vi) 150 m X 60 m extending N40°W - S40°E and, (vii) 130 m X 80 m extending N35°E - S35°W. Quartzite is white, grayish, and greenish and medium to coarse, massive to feebly foliated, and predominantly composed of quartz along with muscovite and opaques (Fig. 2e & 2f). Primary lamination (Fig. 2e & 2f), tabular-cross bedding (Fig. 2g), and trough-cross bedding (Fig. 2h) are also noticed. Basalt is mostly exposed in the hilly terrains which is mesocratic, fine-grained, massive, and consists of plagioclase and pyroxenes as essential minerals along with quartz, magnetite, and sulphides as accessories. Younger intrusives of the study area are represented by dolerite and gabbro dykes (Fig. 1c).

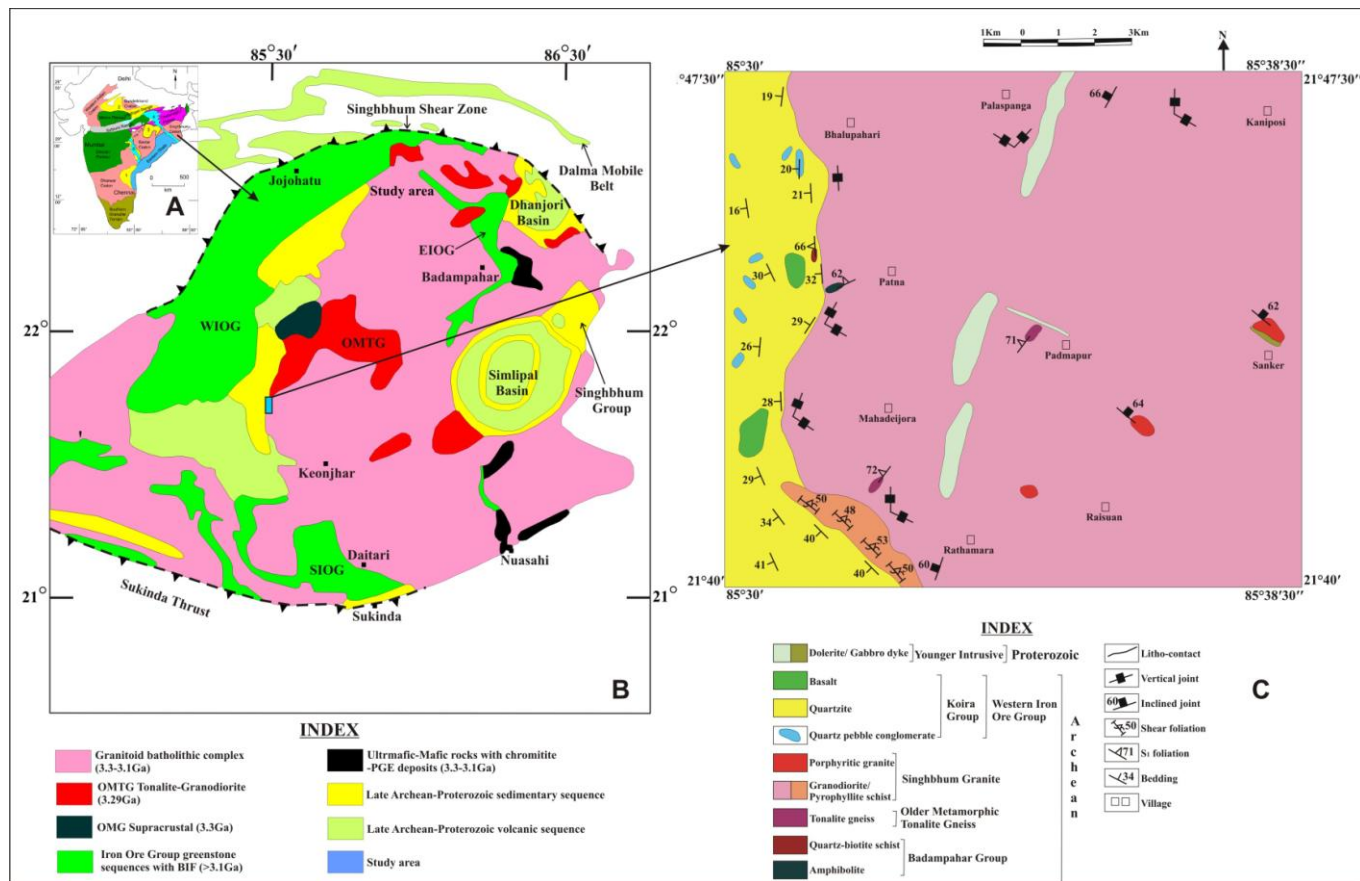


**Figure 1:** Geological maps of study area: (A) Tectonic map of India, (B) Regional geological map of the Singhbhum Craton, north Odisha showing location of the study area (modified after Saha, 1994), and (C) Geological map of the study area showing the occurrence of quartz-pebble conglomerate and quartzite belonging to the Koira Group in parts of Toposheet nos.73G/9 and 73G/10, Kendujhar district, Odisha (modified after Yadav et al., 2016; Yadav and Das, 2019).

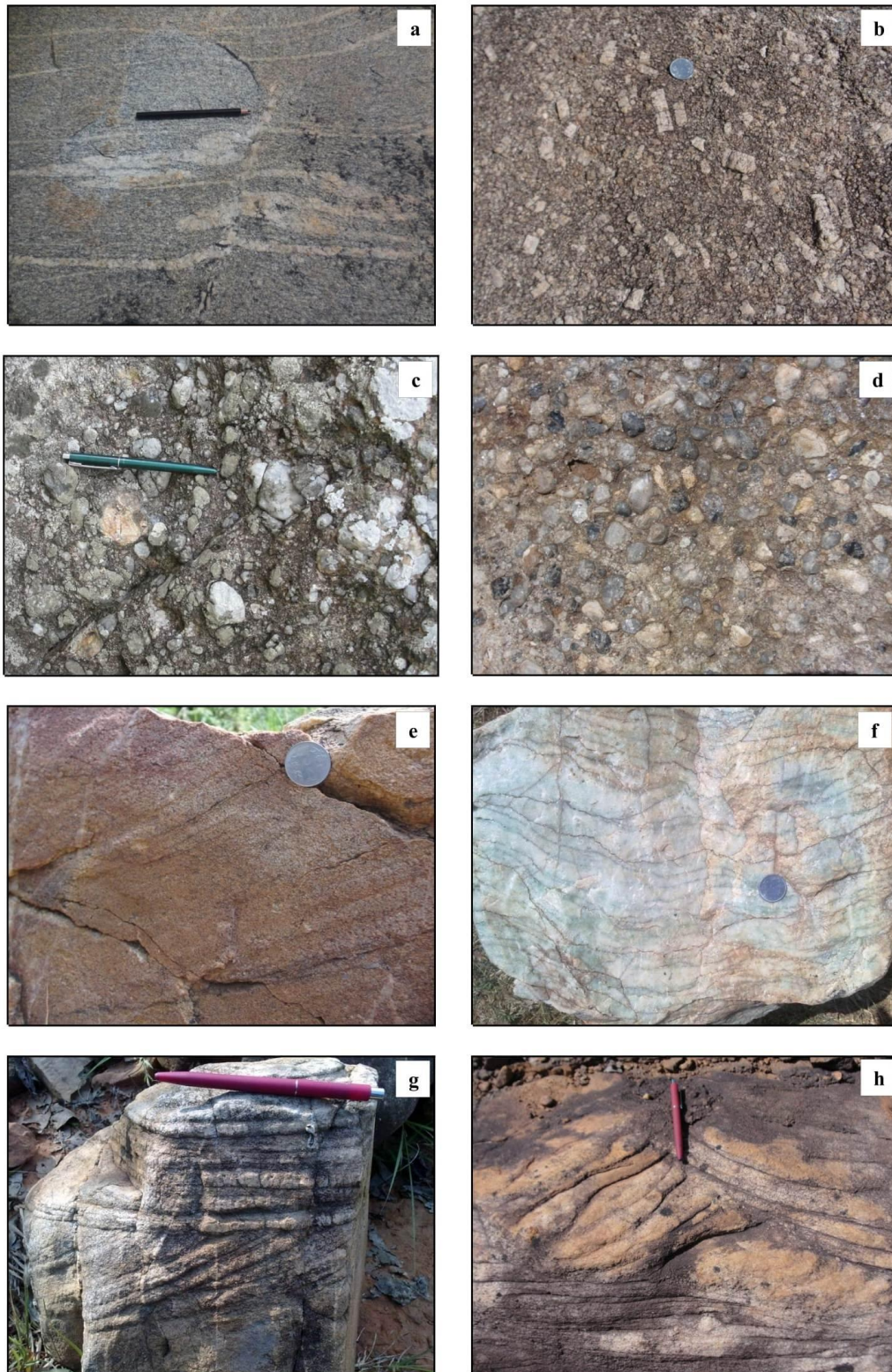


**Figure 2:** (a) Gneissic foliation traversed by numerous quartz and pegmatites veins in tonalite gneiss (b) Phenocrysts of plagioclase and K-feldspar observed within porphyritic granite. (c) Subrounded to subangular clasts of smoky and white quartz embedded in arenaceous matrix of the quartz-pebble conglomerate (d) Clasts of smoky and white quartz within quartz-pebble conglomerate. (e) Primary bedding in ferruginous quartzite of the Koira Group. (f) Colour and compositional banding noticed in quartzite. (g) Tabular-cross bedding within quartzite. (h) Trough-cross bedding in ferruginous quartzite. (Photographs d and e were taken from Yadav and Das, 2019).

### Analytical techniques

15 samples from quartz-pebble conglomerate and quartzite of the Koira Group were collected for analysis of major oxides, trace elements and REE. Major oxides and trace elements were analyzed by X-Ray Fluorescence (XRF) and REE by Inductively Coupled Plasma Mass Spectrometer (ICP-MS) instruments at Geological Survey of India, Eastern Region, Kolkata, India. The analytical data is presented in Table 1.

## 2. Results and Discussion

### 2.1 Geochemical characteristic and classification of QPC and quartzite

Geochemistry of sedimentary rocks can be used to infer source rock composition, weathering, transport history, and depositional conditions of sedimentation (McLennan et al., 1993). Investigations on geochemical characteristics of ancient and modern sediments have been carried out by various workers to infer the source rocks, provenance, and tectonic setting (Bhatia, 1983; Bhatia and Crook, 1986; Roser and Korsch, 1986, 1988; Nesbitt et al., 1996). The major elemental geochemical parameters have been used to define tectonic settings of different sedimentary suites (Bhatia, 1983; Roser and Korsch, 1986). The major oxide concentrations show that the quartz-pebble conglomerates are enriched in SiO<sub>2</sub> content ranging from 82.97 to 94.22 wt. % with an average value of 90.86 wt. %, Al<sub>2</sub>O<sub>3</sub> (1.13 - 9.34 wt. %, average value of 4.58 wt. %), depleted in Na<sub>2</sub>O (0.01 - 0.08 wt. %), CaO (0.06 - 0.10 wt. %), K<sub>2</sub>O (0.17 - 1.34 wt. %), and high TiO<sub>2</sub> (0.1 - 1.09 wt. %). The analytical results of trace elements (Table 1) show some noteworthy values viz., Ba (48 - 1051 ppm), Sr (5 - 50 ppm), Nb (5 - 15 ppm), Cr (132 - 7394 ppm), Rb (5 - 196 ppm), Th (5 - 23 ppm), U (6 - 17 ppm), Y (10 - 26 ppm), V (9 - 186 ppm) and Zr (34 - 485 ppm). Among trace elements, Cr in QPC ranges from 132 to 7394 ppm with an average of 1813.08 ppm which is higher more than eighteen times higher than the Upper Continental Crust (UCC; Krauskopf, 1967; Table 1). The presence of Cr-bearing minerals like fuchsite mica and mafic rock fragments etc., in the QPC matrix accounts for the high Cr values (Yadav and Das, 2019). Values of U, Th, and Y vary from 6 to 17 ppm, 5 to 23 ppm, and 10 to 26 ppm respectively which are distinctly higher than the crustal abundance values. Zirconium (Zr)

value varies from 34 to 485 ppm with an average of 220.33 ppm which is significantly higher than the crustal abundance of Zr (165 ppm). One sample shows higher values of Zr (485 ppm) which is approximately three times higher than the crustal abundance of Zr. Quartzite samples are quite enriched in SiO<sub>2</sub> contents that vary from 89.78 to 91.45 wt. % and Al<sub>2</sub>O<sub>3</sub> vary from 4.23 to 6.53 wt. %. Na<sub>2</sub>O, K<sub>2</sub>O, and CaO contents in quartzite vary from 0.02 to 0.10, 0.85 to 0.95, and 0.02 to 0.06 respectively. TiO<sub>2</sub> content in quartzite ranges from 0.18 to 0.34. The K<sub>2</sub>O/Al<sub>2</sub>O<sub>3</sub> ratio of terrigenous sedimentary rocks was used to decipher the original composition of ancient sediments because the ratio for clay minerals and feldspars are different. The K<sub>2</sub>O/Al<sub>2</sub>O<sub>3</sub> ratio for clay minerals is up to 0.3 and for feldspar, it ranges from 0.3 to 0.9 (Cox et al., 1995). The K<sub>2</sub>O/Al<sub>2</sub>O<sub>3</sub> ratio for QPC ranges from 0.07 to 0.17 with an average of 0.11 and 0.10 to 0.17 (average = 0.14) for quartzites (Tables 1). In both QPC and quartzites, values of K<sub>2</sub>O/Al<sub>2</sub>O<sub>3</sub> ratio indicate the presence of clay minerals and not feldspar which is corroborated by their petrographic characteristics (Yadav and Das, 2019). The potassic nature of QPC and quartzite are reflected by high K<sub>2</sub>O/Na<sub>2</sub>O ratios which range from 11.13 to 37 with an average of 23.88 and 6.50 to 33.50 (average = 16.50) respectively. Low Al<sub>2</sub>O<sub>3</sub>/TiO<sub>2</sub> ratios in QPC compared to quartzites may indicate the presence of Ti-bearing mafic mineral phases like rutile, apatite, zircon, monazite, muscovite, sericite, magnetite, and/or a mixed source (Yadav and Das, 2019).

In binary plot of log (SiO<sub>2</sub>/Al<sub>2</sub>O<sub>3</sub>) vs. log (Na<sub>2</sub>O/K<sub>2</sub>O), QPC samples fall in the field of sub-arkose to sub-litharenite, and few samples come under quartz-arenite field (Fig. 3a; Pettijohn et al., 1972). Most of the samples of quartzites plot in sub-arkose field whereas two samples occupy the field of sub-litharenite (Fig. 3a). In log (SiO<sub>2</sub>/Al<sub>2</sub>O<sub>3</sub>) vs. log (Fe<sub>2</sub>O<sub>3</sub>/K<sub>2</sub>O) plot, four samples of QPC falls in sub-litharenite field and two samples each occupy the field of arkose, sub-arkose and quartz-arenite (Fig. 3b; Heron, 1988) whereas quartzites fall in the field of sub-arkose (Fig. 3b). In the Fe<sub>2</sub>O<sub>3</sub>+MgO-Na<sub>2</sub>O-K<sub>2</sub>O triangulation plot, most of the samples of QPC occupying the composition of ferromagnesian potassic sandstones except few sample falls in the field of potassic sandstones (Fig. 3c). Quartzite shares both the field of ferromagnesian potassic sandstones and potassic sandstones (Fig. 3c; Naqvi et al., 1980).

**Table 1:** Major elements (in %), trace elements and REE values (in ppm) data of quartz-pebble conglomerates and quartzite from the Koira Group, Singhbhum Craton

Sample Nos.	CK-1	CK-2	CK-3	CK-4	CK-5	CK-6	CK-7	CK-8	CK-9	CK-10	QK-1	QK-2	QK-3	QK-4	QK-5
Major oxides (wt. %)	Quartz-pebble conglomerate										Quartzite				
SiO <sub>2</sub>	85.9	92.15	82.97	90.2	93.71	94.22	91.83	93.11	90.91	93.61	90.26	89.78	90.23	91.45	90.79
TiO <sub>2</sub>	0.24	0.14	1.09	0.54	0.12	0.1	0.35	0.35	0.52	0.13	0.23	0.34	0.24	0.2	0.18
Al <sub>2</sub> O <sub>3</sub>	9.34	4.91	9	1.13	3.92	3.85	4.23	2.75	1.43	5.23	5.45	6.53	5.4	4.23	5.1
Fe <sub>2</sub> O <sub>3</sub> (T)	1.04	0.39	0.41	6.42	0.68	0.25	1.62	2.17	5.97	0.46	0.45	0.51	0.25	0.58	0.31
MgO	0.36	0.13	0.28	0.03	0.04	0.04	0.16	0.15	0.03	0.08	0.23	0.26	0.15	0.13	0.12
MnO	0.01	0.01	0.01	0.03	0.01	0.01	0.02	0.01	0.02	0.01	0.05	0.02	0.02	0.03	0.02
CaO	0.06	0.06	0.09	0.1	0.07	0.06	0.07	0.08	0.1	0.06	0.05	0.04	0.02	0.06	0.04
Na <sub>2</sub> O	0.08	0.06	0.07	0.01	0.01	0.01	0.01	0.01	0.01	0.01	0.09	0.02	0.06	0.05	0.1
K <sub>2</sub> O	0.89	0.79	1.34	0.19	0.27	0.35	0.37	0.26	0.17	0.34	0.95	0.89	0.92	0.85	0.91

P <sub>2</sub> O <sub>5</sub>	0.03	0.02	0.03	0.09	0.03	0.03	0.04	0.04	0.08	0.02	0.04	0.06	0.03	0.02	0.03
Total	97.95	98.66	95.29	98.74	98.86	98.92	98.7	98.93	99.24	99.95	97.8	98.45	97.32	97.6	97.6
Trace elements and REE (ppm)															
Ba	425	168	1051	359	106	128	172	48	212	130	365	289	136	110	104
Co	5	10	7	5	5	5	8	6	5	6	4	7	8	10	5
Cr	181	760	1240	968	432	132	7394	839	1098	1187	154	306	89	134	149
Cu	19	8	49	5	5	5	5	5	5	5	4	8	4	7	10
Ga	11	7	22	6	9	7	8	8	7	8	5	8	9	11	14
Nb	6	5	13	14	6	5	15	8	13	5	4	9	11	6	8
Ni	5	6	8	15	8	5	10	24	28	13	4	20	9	11	17
Pb	8	13	9	73	5	5	15	5	48	6	67	20	8	6	17
Rb	54	19	196	5	5	8	25	15	11	23	9	54	48	27	41
Sc	5	5	10	5	5	5	5	5	5	5	2	4	6	2	5
Sr	5	5	50	18	13	15	5	5	17	5	5	11	17	9	19
Th	8	5	14	18	6	5	18	21	23	6	11	4	9	6	3
U	7	6	8	15	9	9	15	17	12	8	5	6	2	6	4
V	29	17	186	28	9	10	37	18	37	15	9	13	8	15	11
Y	14	10	25	25	13	13	13	14	26	12	9	7	8	5	9
Zn	13	22	15	32	14	13	11	21	12	15	10	7	11	8	12
Zr	108	69	485	275	104	85	34	224	352	389	114	260	87	160	213
La	146.85	122.23	156.93	202.02	165.76	183.22	201.44	178.99	164.22	198.44	87.45	98.40	84.78	110.23	98.25
Ce	281.54	229.30	291.59	345.33	293.55	245.77	367.90	245.08	281.33	354.76	123.45	110.23	106.34	167.34	138.79
Pr	35.11	28.87	39.61	44.97	23.65	25.78	45.88	45.77	36.44	36.77	7.56	8.45	6.45	2.67	2.58
Nd	125.03	103.39	143.28	160.37	150.22	132.78	170.44	189.70	132.66	198.45	28.89	21.34	22.45	18.89	21.34
Sm	22.30	19.18	28.52	29.61	24.56	16.75	17.98	29.56	17.68	18.66	8.44	7.45	6.33	4.55	6.78
Eu	3.97	3.64	3.54	4.74	2.55	3.97	4.74	3.52	3.67	4.66	4.23	1.00	0.50	0.89	1.50
Gd	24.89	21.37	31.11	33.44	24.87	19.55	35.21	38.95	25.77	25.78	7.46	6.56	4.46	3.45	3.56
Tb	3.47	3.09	4.83	4.70	5.78	3.78	4.90	2.97	4.70	4.90	3.56	1.35	2.55	1.50	1.78
Dy	20.12	17.77	28.53	27.36	25.76	26.86	25.99	26.88	24.99	28.79	12.56	11.47	8.79	11.67	10.78
Ho	3.76	3.40	5.38	5.23	2.76	2.45	5.23	3.00	3.55	3.45	1.34	1.23	1.57	1.03	1.70
Er	11.29	10.35	16.25	15.94	1.21	9.56	18.99	19.70	8.45	9.44	2.95	3.56	2.45	2.67	2.58
Tm	1.85	1.70	2.65	2.61	3.56	1.67	2.61	1.77	2.55	2.61	1.56	1.49	0.89	1.45	0.98
Yb	11.53	10.45	15.97	16.42	1.25	14.24	14.76	15.30	9.88	17.66	6.70	5.89	3.56	2.45	3.15
Lu	1.86	1.64	2.38	2.57	2.54	1.62	1.45	1.76	1.88	2.78	1.45	0.40	1.34	1.56	1.89
ΣREE	693.58	576.37	770.55	895.29	728.02	688.0	917.51	802.96	717.77	907.15	297.60	278.82	252.46	330.35	295.66
ΣLREE	614.79	506.60	663.46	787.04	660.29	608.27	808.38	692.62	636.00	811.74	260.02	246.87	226.85	304.57	269.24
ΣHREE	78.78	69.77	107.09	108.25	67.73	79.73	109.13	110.33	81.77	95.41	37.58	31.95	25.61	25.78	26.42
Average	49.54	41.17	55.04	63.95	52.00	49.14	65.54	57.35	51.27	64.80	21.26	19.92	18.03	23.6	21.1
LREE/HREE	7.80	7.26	6.20	7.27	9.75	7.63	7.41	6.28	7.78	8.51	6.92	7.73	8.86	11.81	10.19
Eu/Eu*	0.52	0.55	0.36	0.46	0.32	0.67	0.58	0.32	0.53	0.65	1.63	0.44	0.29	0.69	0.93
(La/Sm) <sub>N</sub>	4.14	4.01	3.46	4.29	4.25	6.88	7.05	3.81	5.84	6.69	6.52	8.31	8.42	10.4	9.12
(La/Yb) <sub>N</sub>	8.58	7.89	6.63	8.30	9.12	8.67	9.20	7.89	11.21	7.58	8.80	11.26	16.06	30.3	21.3
(Gd/Yb) <sub>N</sub>	1.74	1.65	1.57	1.64	1.45	1.11	1.93	2.05	2.10	1.18	0.90	0.90	1.01	1.14	0.91
Co+Cr+Sc	191	775	1266	978	442	142	7407	850	1108	1198	160	317	103	146	159
La+Th+U	161.8	133.2	178.9	235	180.7	197.2	234.4	216.9	199.2	212.4	103.4	108.4	95.7	122	105
Zr/Y	7.71	6.90	19.40	11.00	8.00	6.54	2.62	16.00	13.54	39.69	12.67	37.14	10.88	32	23.7
La/Sc	29.37	24.45	8.26	40.40	33.15	36.64	40.29	35.80	32.84	39.69	43.73	24.60	14.13	55.1	19.6
Th/Sc	1.60	1.00	1.40	3.60	1.20	1.00	3.60	4.20	4.60	1.20	5.50	1.00	1.50	3.00	0.60
Th/U	1.14	0.83	1.75	1.20	0.67	0.56	1.20	1.24	1.92	0.75	2.20	0.67	4.50	1.00	0.75
K <sub>2</sub> O/Na <sub>2</sub> O	11.13	13.17	19.14	19.00	27.00	35.00	37.00	26.00	17.00	34.00	10.56	33.50	15.33	9.60	6.50
K <sub>2</sub> O+Na <sub>2</sub> O	0.97	0.85	1.41	0.20	0.28	0.36	0.38	0.27	0.18	0.35	1.04	0.69	0.98	0.53	0.75
K <sub>2</sub> O/Al <sub>2</sub> O <sub>3</sub>	0.10	0.16	0.15	0.17	0.07	0.09	0.09	0.09	0.12	0.07	0.17	0.10	0.17	0.11	0.13
Fe <sub>2</sub> O <sub>3</sub> /MgO	2.89	3	1.46	214	17	6.25	10.13	14.47	199	5.75	1.96	1.96	1.67	4.46	2.58
Fe <sub>2</sub> O <sub>3</sub> +MgO	1.40	0.52	0.69	6.45	0.72	0.29	1.78	2.32	6.00	0.54	0.68	0.77	0.40	0.71	0.43
Al <sub>2</sub> O <sub>3</sub> /TiO <sub>2</sub>	38.92	35.07	8.26	2.09	32.67	38.50	12.09	7.86	2.75	40.23	23.70	19.21	22.50	21.1	28.3
CIA	88.58	82.35	84.26	82.57	92.34	90.34	90.71	89.74	86.83	92.88	80.45	89.20	81.90	86.1	83.1
PIA	97.21	95.36	97.04	96.56	99.10	99.06	99.15	98.68	97.43	99.33	93.72	98.88	95.71	95.7	93.1

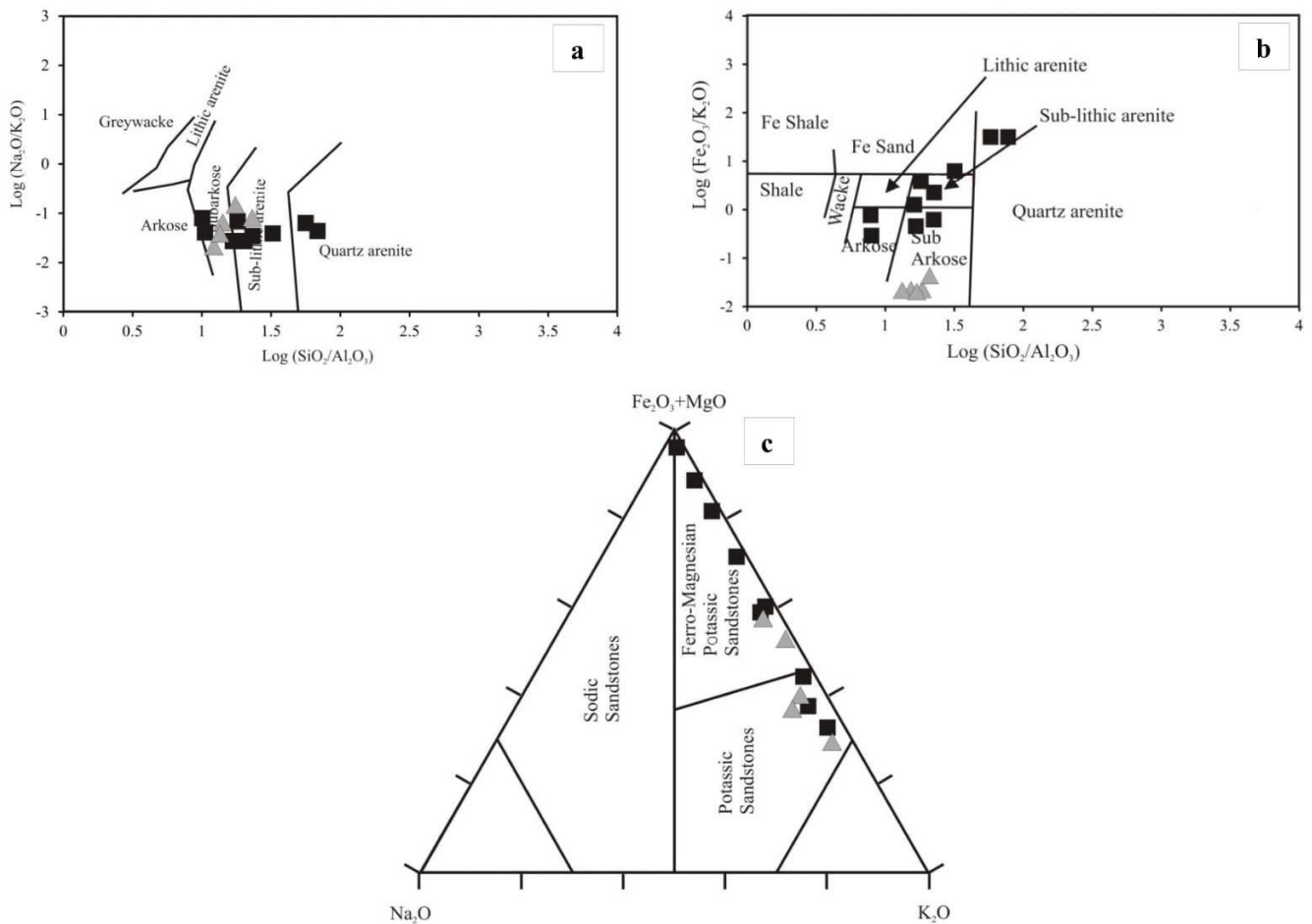


**Figure 3:** (a) Chemical classification of QPC and quartzites on log (SiO<sub>2</sub>/Al<sub>2</sub>O<sub>3</sub>) vs. log (Na<sub>2</sub>O/K<sub>2</sub>O) diagram after Pettijohn et al., 1972. (b) Log (SiO<sub>2</sub>/Al<sub>2</sub>O<sub>3</sub>) vs. Log (Fe<sub>2</sub>O<sub>3</sub>/K<sub>2</sub>O) diagram was used for classification of QPC and quartzite. QPC falls in sub-litharenite, arkose, sub-arkose and quartz- arenite fields respectively whereas quartzites occupy the field of sub-arkose. (c) Fe<sub>2</sub>O<sub>3</sub>(T)+MgO-Na<sub>2</sub>O-K<sub>2</sub>O triangular plot was used for classification of the clastic rocks. (Symbols used in plots: ■ - Quartz-pebble conglomerate; ▲ - Quartzite).

### Provenance

Geochemistry provides important information in provenance determination especially for the fine-grained sedimentary rocks (McLennan et al. 1993). Trace elements (Zr, Y, Sc, Nb, Th, and REE) in clastic sedimentary rocks are considered to be immobile during weathering, diagenesis, and low to moderate grade of metamorphism, and their signatures are commonly preserved in sedimentary rocks (Bhatia and Crook, 1986). Hence, the trace elements ratios are most suited elements for provenance and tectonic setting determinations because of their relatively lower mobility during sedimentary processes/subsequent alteration and their low residence time in seawater (Holland, 1984; Bhatia and Crook, 1986; McLennan et al., 1993; Nesbitt et al., 1996; McLennan, 2001). The trace element concentrations and elemental ratios are presented in Table 1. The samples of QPC and quartzite are plotted in the bivariate diagram of TiO<sub>2</sub> vs. Zr in which all the samples fall in the felsic igneous rocks (Fig. 4a). QPC and quartzite samples occupy the granites and gneisses field while plotted in the discriminant function diagram (Fig. 4b, P1-Felsic Igneous Provenance; P2 - Intermediate Igneous

Provenance; P3 - Mafic Igneous Provenance, and P4 - Granites and Gneisses; Roser and Korsch, 1988). It is corroborated that the sediments derived from granites and gneisses for the formation of QPC- quartzite sequence in the study area. Felsic provenance for the QPC and quartzites is also confirmed by the plot of TiO<sub>2</sub> vs. Ni (Fig. 4c; Floyd et al., 1989). In Th/U vs. Th diagram, all the samples of QPC and quartzites occupy the field of depleted mantle source, indicating uranium enrichment and reducing environment during the time of weathering and deposition of sediments.

Most of the sandstone or quartzite in Archean greenstone belts are showing REE pattern, similar to the typical average of the Post Archean Australian Shale (PAAS). The REE patterns have also been used to infer sources of sedimentary rocks, since basic rocks contain low LREE/HREE ratios whereas more silicic rocks usually contain higher LREE/ HREE ratios and negative Eu anomalies (Cullers and Graf, 1983; Taylor and McLennan, 1985; Wronkiewicz and Condie, 1987, 1989). McLennan and Taylor (1991) and Taylor and McLennan (1985) have interpreted the value of Eu anomaly in

sedimentary rocks are mainly related to igneous source rocks. Negative Eu anomalies in the sedimentary rocks are indicated that the possible provenance is derived by intracrustal differentiation processes (Ghosh et al., 2016). Generally, the Archean sediments show no or only very slight Eu depletion. In the Archean terrain, negative Eu anomalies are reported from sediments of the Pongola Supergroup, the Kaapvaal craton, South Africa, West Greenland, and Abitibi greenstone belt, Canada (Taylor and McLennan, 1985; Wronkiewicz and Condie, 1989; Condie and Wronkiewicz, 1990; Feng and Kerrich, 1990). REE plot of QPC exhibit enrichment of LREE with almost flat HREE, due to the presence of epidote, allanite, apatite, zircon, and monazite grains was observed from the petrographic study (Yadav and Das, 2019) whereas the REE are relatively fractionated in quartzites with depleted HREE (Fig. 4e & 4f). (La/Sm)<sub>N</sub> values ranging from 3.46 to 7.05 in QPC and 6.52 - 10.2 in quartzite, and (Gd/ Yb)<sub>N</sub> values

ranging from 1.1 to 2.10 in QPC and 0.90 - 1.14 in quartzite which are attributed the LREE enrichment in QPC and quartzite. Fractionate REE value of (La/Yb)<sub>N</sub> is noticed in both QPC and quartzite which vary from 6.63 to 11.21 in QPC and 8.80 - 30.33 in quartzites. Eu anomaly in QPC and quartzite varies from 0.32 to 0.67 and 0.29 - 1.63 respectively which is attributed to the presence of Eu depleted felsic igneous rocks in the provenance such as granites. QPC is generally characterized by significant depletion of Eu in Chondrite normalised REE pattern, the higher concentration of total REE, and increase in Th/Sc ratio (Bhushan and Sahoo, 2010). High Th, U, Zr, La, and Ce values together with fractionated Chondrite normalized REE pattern and negative Eu anomaly suggest granitic provenance for the sequence of QPC and quartzite in the study area.

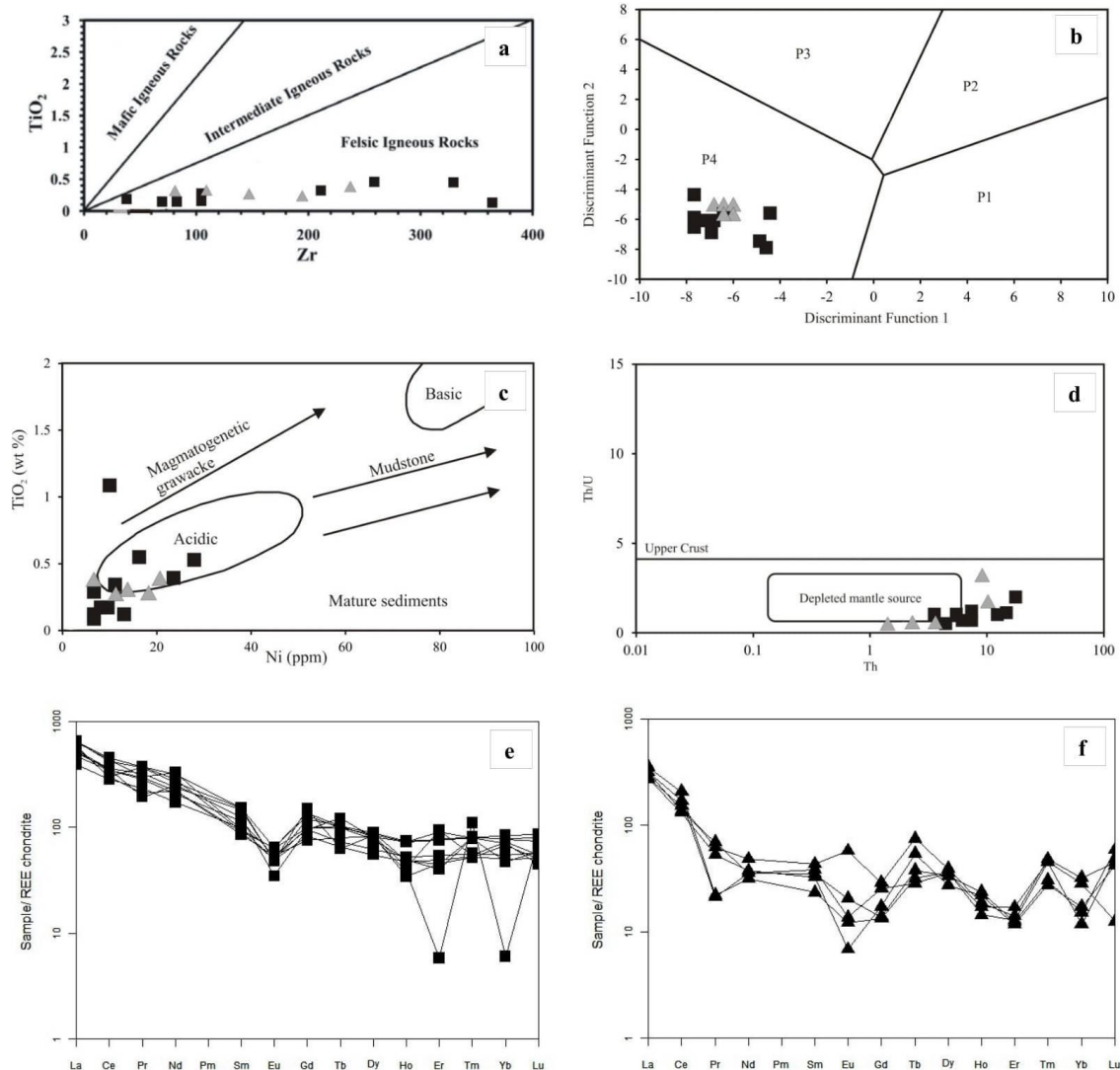


**Figure 4:** (a) TiO<sub>2</sub> vs. Zr plot is used to predict the precursor rocks of QPC and quartzite (Hayashi et al., 1997). (b) Possible provenance for QPC and quartzites are depicting through discriminant function, DF-1 vs. DF-2 plot (Roser and Korsch, 1988; DF-1= (-1.773×TiO<sub>2</sub>) + (0.607×Al<sub>2</sub>O<sub>3</sub>) + (0.76×Fe<sub>2</sub>O<sub>3</sub>) - (1.5×MgO) + (0.616×CaO) + (0.509×Na<sub>2</sub>O) - (1.224×K<sub>2</sub>O) - 9.09; DF-2 = (0.445×TiO<sub>2</sub>) + (0.07×Al<sub>2</sub>O<sub>3</sub>) - (0.25×Fe<sub>2</sub>O<sub>3</sub>) - (1.142×MgO) + (0.438×CaO) + (1.475×Na<sub>2</sub>O) + (1.426×K<sub>2</sub>O) - 6.861. (c) TiO<sub>2</sub> vs. Ni diagram is selected for identifying the provenance of QPC and quartzites (Floyd et al., 1989) (d) QPC and quartzites

representing low Th/U ratios suggesting the enrichment of uranium as seen from the Th/U vs. Th diagram (McLennan et al., 1993). (e & f) Chondrite normalized REE patterns of QPC and quartzite showing fractionation of LREE, strong negative Eu anomaly and flat HREE patterns. (Symbols as in Fig. 3).

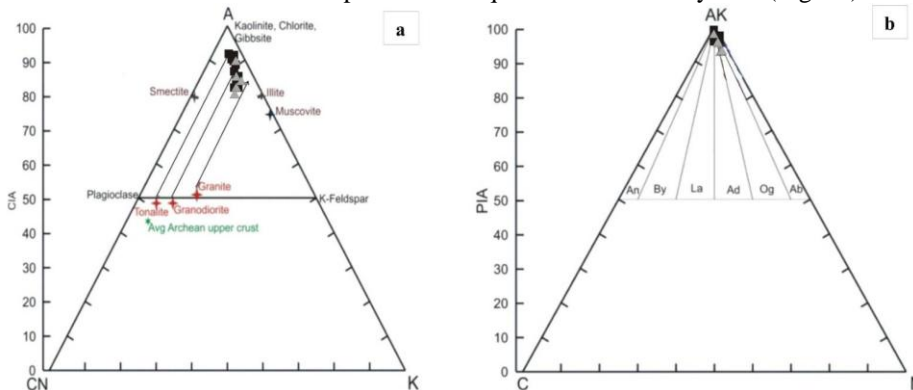
### Paleo-weathering and depositional environment

Paleo-weathering history can be reconstructed based on various geochemical parameters. The degree of chemical weathering and the nature of source rock for sediments can be assessed by knowing the Chemical Index of Alteration (Nesbitt and Young, 1982, 1984). The weathering history of the source rock has been deduced from the quantitative measurement of chemical weathering of silicates by calculating the Chemical Index of Alteration (CIA) and Plagioclase Index of Alteration (PIA) by Nesbitt and Young, 1982, 1984; Fedo et al., 1995; Akarish and EL-Gohary, 2011. The CIA represents a ratio of predominantly immobile  $Al_2O_3$  to the mobile cations  $Na^+$ ,  $K^+$ , and  $Ca^{2+}$  given as oxides. The CIA is defined as  $CIA = [Al_2O_3 / (Al_2O_3 + CaO^* + Na_2O + K_2O)] \times 100$  in molecular proportions and  $CaO^*$  is the amount incorporated in the silicate fraction of the rock. The values of the CIA reflect the intensity of chemical weathering in the source region (Nesbitt and Young, 1982). Fedo et al. (1995) proposed that the CIA value of 50 - 60 indicates an incipient weathering, CIA 60 - 80 intermediate weathering, and CIA >80 extreme weathering. The degree of chemical weathering can also be estimated by using the PIA in molecular proportions and the PIA can be worked out as  $PIA = (Al_2O_3 - K_2O) / (Al_2O_3 + CaO^* + Na_2O - K_2O) \times 100$ , where  $CaO^*$  is CaO only reside in silicate fractions (Fedo et al., 1995).

The values of the CIA in QPC (n = 10) vary from 82.35 to 92.88, and for quartzites, this value shows variation from 80.45 to 89.20 (Table 1). Based on the CIA values, a high degree of chemical weathering was depicted in the sequence of QPC and quartzite of the study area. In the A-CN-K diagram, the majority of the QPC and quartzite samples cluster along the A-K line in between kaolinite-illite field which also indicates the weathering trend of granite, granodiorite, and tonalite are shown at the base of the plagioclase-K-feldspar line (Fig. 5a). These trend lines and points on A-CN-K diagram when traced back provide information about the source of the sedimentary suites. The majority of samples of QPC and quartzite fall between the granodiorite and tonalite fields which indicate the probable

source for the QPC-quartzite sequence (Fig. 5a) which is also corroborated by the presence of different types of granitic rocks ranging from granodiorite to tonalite in the study area (Fig. 1c). The values of PIA for QPC ranges from 95.36 to 99.33 while for quartzites, range varies from 93.08 to 98.88 which reveals that the high degree of plagioclase alteration and their complete dissolution (Table 1). In AK-C-N ternary diagram, all the samples of QPC and quartzites falls between oligoclase (Olg) and albite (Ab) fields (Fig. 5b) which attributes that the plagioclase was completely altered.

The sequence of QPC and quartzite predominantly consists of fluvial quartz-pebble conglomerates and pebbly sandstones that grade upward to the thick mature quartz arenite of shallow-shelf origin. The sandstone is dominantly composed of well-sorted medium to fine-grained mature arenitic sandstone beds. This lithofacies is generally 1 to 3 m thick and shows the development of three subfacies which are associated with variable combination to form Fining Upward (FU) cycles. Tabular-cross bedding is exhibited by fine to medium-grained, moderately sorted sandstone which is characterized by thick cross bed sets having thickness varies from 15 to 25 cm with the low foreset inclination of  $10^\circ$  to  $15^\circ$ . The topset, foreset, and bottom set range in thickness from 20 to 50 cm (see Fig. 2g). The tabular-cross bedding is formed by the migration of 2D bedforms which indicates high energy and large sediment influx (Allen, 1980). Large scale trough-cross is dominated by large trough sets which ranges in thickness from 1 to 1.5 m. It is developed in iron pigmented red, medium-grained sandstone, and is characterized by thick cross bed sets capped by thin siltstone layers (Fig. 2h). Large scale trough-cross is mainly formed by migration of 3D bedforms or dunes in shallow water conditions indicate deposition in the sub-tidal environment (Mowbray and Visser, 1984). Palaeocurrent directions are preferably collected from tabular-cross bedding and trough-cross bedding respectively which varies from  $280^\circ$  to  $310^\circ$ . A bivariate plot of  $SiO_2$  versus total  $Al_2O_3 + K_2O + Na_2O$  as proposed by Suttner and Dutta (1986) was used to identify the climatic conditions for the formation of the QPC and quartzite sequence (Fig. 5c). Semi-humid condition was responsible for the formation of QPC and quartzite of the study area (Fig. 5c).



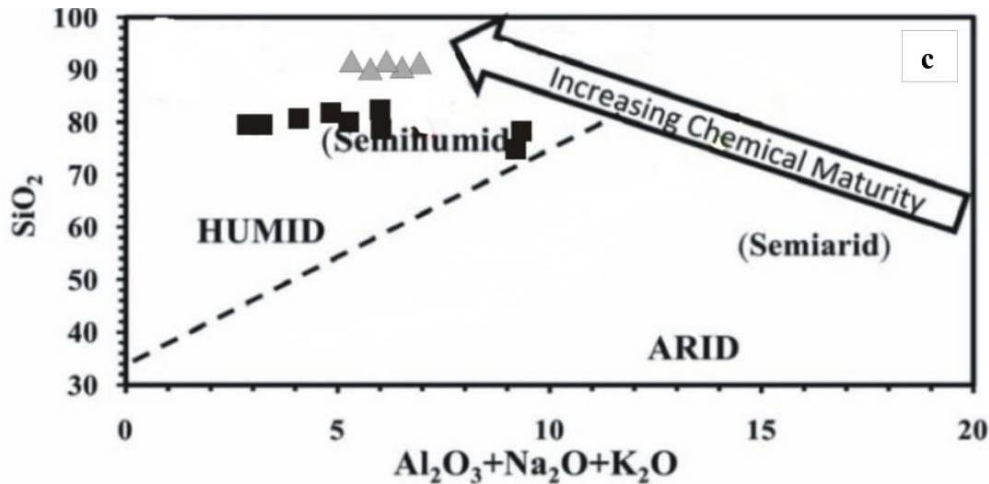
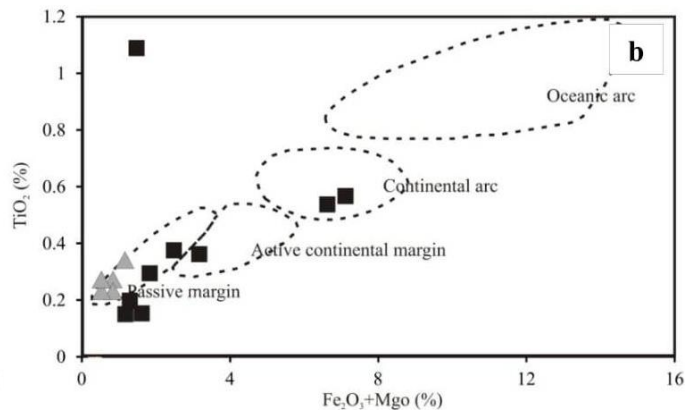
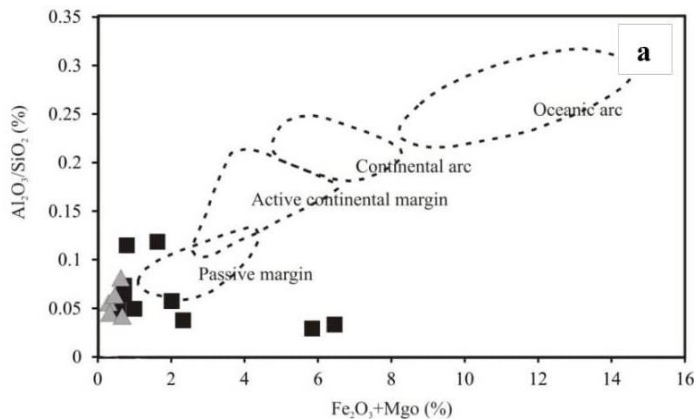


**Figure 5:** (a) A-CN-K ( $Al_2O_3$ - $CaO^*$ + $Na_2O$ - $K_2O$ ) ternary diagram (Nesbitt and Young, 1982) and the arrow shows the trend of weathering and alteration (Condie, 1993) used in which majority of the QPC and quartzite samples cluster along the A-K line in between kaolinite-illite field. (b) QPC and quartzites samples occupy the fields of alkali feldspar in the AK-C-N ternary diagram (Fedo et al., 1995). (c) Chemical maturity of the QPC and quartzites depicted from the bivariate plot of  $SiO_2$  vs.  $Al_2O_3+K_2O+Na_2O$  field (Suttner and Dutta, 1986). (Symbols as in Fig. 3 and 4).

**Tectonic setting**

The Archean tectonics was not like present-day plate tectonics and many other workers believe that plate tectonics have been active since the Paleo-Mesoarchean (Kato et al., 1998; Vearncombe and Kerrich, 1999; Smithies et al., 2005; Condie, 2006; Garde, 2007; Taylor and McLennan, 2009; Bastow et al., 2011; Mukhopadhyay et al., 2012; Hamilton, 2013). Siliciclastic successions composed of mature sandstones and shales occurring unconformably on an older basement do exist in the Archean, and they could be remnants of passive margin successions viz., Moodies Supergroup in South Africa; the Pongola Supergroup in South Africa; the Narryer Complex and the Mount Bruce Supergroup in Western Australia; the Bababudan Group in southern India; the Canadian Shield; southern Zimbabwe (Eriksson, 1978; Srinivasan and Ojakangas, 1986; Wronkiewicz and Condie, 1989; Lowe, 1994; Fedo and Eriksson, 1996; Donaldson and de Kemp, 1998). Major elemental compositions and certain trace element ratios including REE were also used by different workers to decipher provenance study and tectonic setting of the sedimentary rocks (Bhatia, 1983; Taylor and McLennan, 1985; Roser and Korsch, 1986; McLennan, 1989; McLennan and Taylor, 1991; Cullers, 1994, 2000).

The common discrimination diagrams like  $Al_2O_3/SiO_2$  vs.  $Fe_2O_3+MgO$  and  $TiO_2$  vs.  $Fe_2O_3+MgO$  after Bhatia (1983) was used for depicting the tectonic setting of QPC and quartzite. In  $Al_2O_3/SiO_2$  vs.  $Fe_2O_3+MgO$  diagram, all the samples fall near the passive margin tectonic setting (Fig. 6a) whereas most of the samples of QPC and quartzite occupy the passive margin field except few samples fall in the active continental margin and continental arc fields, depicted from the diagram of  $TiO_2$  vs.  $Fe_2O_3+MgO$  (Fig. 6b; Bhatia 1983). In  $SiO_2$  vs.  $K_2O/Na_2O$  plot of Roser and Korsch (1986), all the samples of QPC and quartzites occupy the field of passive margin tectonic setting (Fig. 6c). Majority of the QPC and quartzite samples occupy the passive margin setting (Fig. 6d & 6e) while plotted in the ternary diagram of  $CaO$ - $N_2O$ - $K_2O$  (Bhatia, 1983), and  $SiO_2/20$ - $K_2O+Na_2O$ - $TiO_2+Fe_2O_3(t)+MgO$  (Kroonberg, 1994). In La-Th-Sc ternary diagram, the QPC and quartzite falls near active continental margin and passive margin fields (Fig. 6f; Bhatia and Crook, 1986). The provenance of a mixture of dominantly felsic recycled material with a minor mafic source for QPC and quartzite was depicted from the Th-Sc-Zr/10 ternary plot (Bhatia and Crook, 1986).



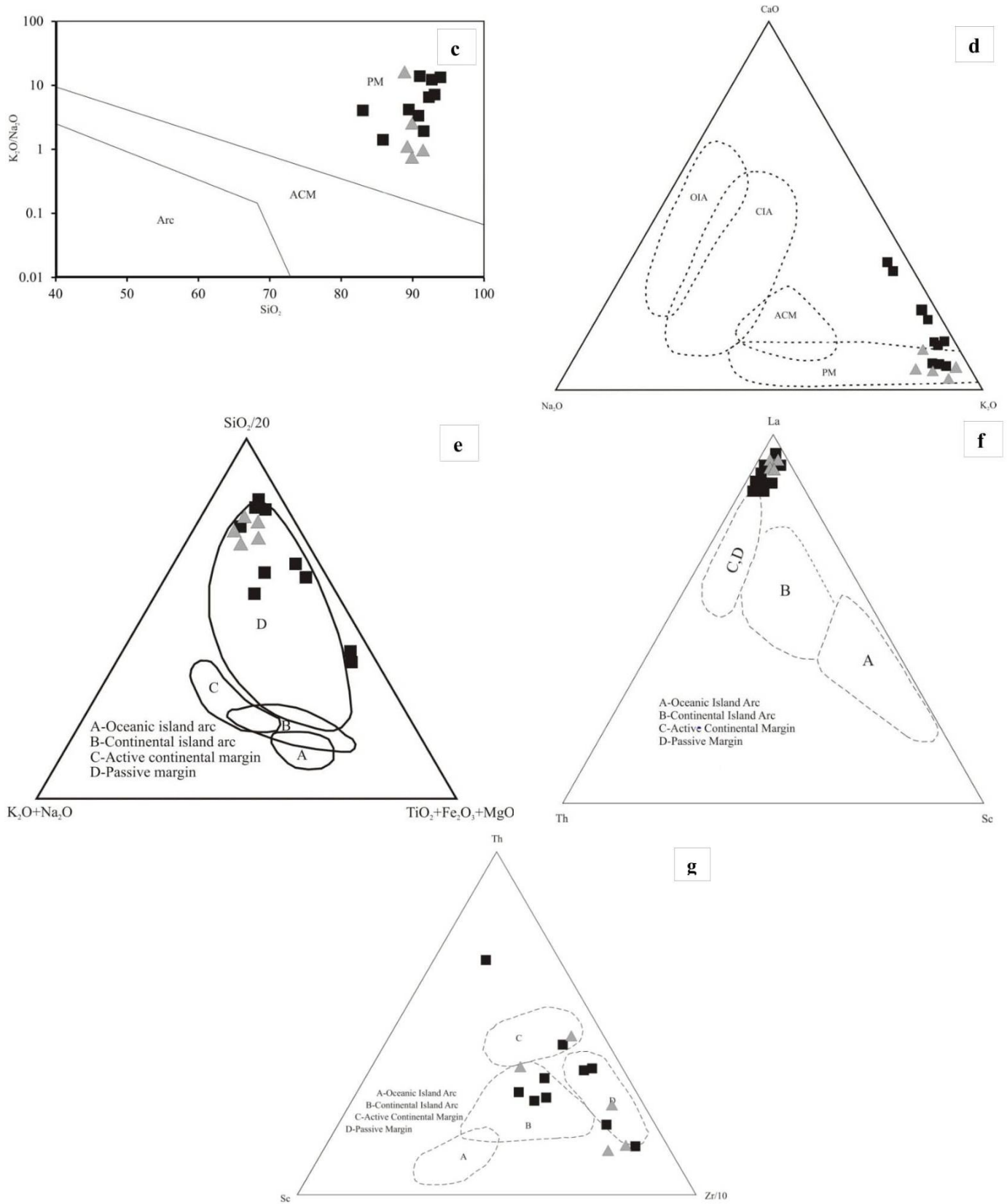


**Figure 6:** (a) QPC and quartzite samples fall close to the passive margin tectonic setting as seen in plot of  $\text{Fe}_2\text{O}_3+\text{MgO}$  vs.  $\text{Al}_2\text{O}_3/\text{SiO}_2$  (Bhatia, 1983). (b)  $\text{Fe}_2\text{O}_3(\text{T})+\text{MgO}$  vs.  $\text{TiO}_2$  plot used for depicting the tectonic setting of QPC and quartzite (Bhatia, 1983). (c)  $\text{K}_2\text{O}/\text{Na}_2\text{O}$  vs.  $\text{SiO}_2$  plot of QPC and quartzites displaying passive margin setting (Roser and Korsch, 1986). (d & e) Ternary diagram of  $\text{CaO}-\text{Na}_2\text{O}-\text{K}_2\text{O}$  (Bhatia, 1983) and  $\text{SiO}_2/20-\text{K}_2\text{O}+\text{Na}_2\text{O}-\text{TiO}_2+\text{Fe}_2\text{O}_3(\text{t})+\text{MgO}$  (Kroonberg, 1994) used for

depicting the tectonic setting of QPC and quartzite. Most of the samples of these units fall in passive margin setting. (f) Samples of QPC and quartzites plotted in the ternary diagram of La-Th-Sc in which all the samples falls near the boundary of active continental margin and passive margin fields. (g) Th-Sc-Zr/10 ternary plot showing mixed type of tectonic setting for QPC and quartzite (Bhatia and Crook, 1986). (Symbols as in Fig. 4 and 5).

### 3. Conclusion

High degree of CIA and PIA values are noticed in the QPC and quartzite sequence at the eastern fringe of the western Iron Ore Group and the Singhbhum Granite which is exposed in the western margin of Singhbhum Craton in Kendujhar district, Odisha. CIA study suggested that the granodiorite and tonalite are the possible provenance source for the QPC and quartzite. Besides, the major oxides, trace elements including REE, trace elements ratios, binary, and ternary plots are also used for depicting the provenance and tectonic setting of QPC and quartzite sequence. All the data indicates that these sediments have been mostly derived from felsic igneous rocks which are ranging from granodiorite to tonalite with a minor contribution from mafic and ultramafic sources. In addition, the values of Pb, U, Th, Y, La, Ce, and low Sc with high critical trace elemental ratios of Th/U, Th/Sc, Zr/Y, and La/Sc in QPC indicates their derivation from the felsic igneous source. Low concentration of Th and Sc, and variable ratios of Th/Sc is attributed to the mixed source both felsic and mafic for the derivation of quartzite. Geochemical studies further suggest that QPC and quartzite have been deposited in a passive margin tectonic setting developed during Archean along the western margin of Singhbhum Craton corroborated by their high  $\text{SiO}_2/\text{Al}_2\text{O}_3$  ratios, LREE enrichment, and Th/U, Th/Sc, Zr/Y, and La/Sc ratios.

### 4. Acknowledgments

Authors are extremely indebted to the Director General, Geological Survey of India for permitting to publish the paper. They are also greatly obliged to the Deputy Director General, Geological Survey of India, SU: Bihar for constant cooperation, encouragement, guidance, and valuable suggestions during the work.

### References

- [1] Akarish, A.I.M. and EL-Gohary, A.M. (2011) Provenance and source area weathering derived from the geochemistry of Pre-Cenomanian sandstones, east Sinai. *Egypt Jour. Appl. Sci.*, v.11(17), pp.3070-3088.
- [2] Allen, J.R.L. (1980) Sand waves: a model of origin and internal structures. *Sedi. Geol.*, v.26, pp.281-328.
- [3] Banerjee, P.K. (1982) Stratigraphy, petrology and geochemistry of some Precambrian basic volcanic and associated rocks of Singhbhum district, Bihar and Mayurbhanj and Keonjhar districts, Orissa. *Mem. Geol. Surv. India*, v.111, pp.1-54.
- [4] Basu, A., Santanu, S. and Bhowmik, K. (2008) Constraining the metamorphic evolution of a cryptic hot Mesoproterozoic orogen in the Central Indian Tectonic Zone, using P-T pseudosection modeling of mafic intrusions and host reworked granulites. *Precamb. Res.*, v.162(1-2), pp.128-149.
- [5] Bastow, I.D., Thompson, D.A., Wookey, J., Kendall, J.M., Helffrich, G., Snyder, D.B., Eaton, D.W. and Darbyshire, F. (2011) Precambrian plate tectonics: seismic evidence from northern Hudson Bay, Canada. *Geology*, v.39(1), pp.91-94.
- [6] Bergen, L. and Fayek, M. (2012) Petrography and geochronology of the Pele Mountain quartz pebble conglomerate uranium deposit, Elliot Lake District. *Canada Amer. Min.*, v.97, pp.1274-1283.
- [7] Bekker, A., Holland, H.D., Wang, P.L., Rumble, D., Stein, H.J., Hannah, J.L., Coetsee, L.L. and Beukes, N.J. (2004) Dating the rise of atmospheric oxygen. *Nature*, v.427, pp.117-120.
- [8] Bhatia, M.R. (1983) Plate tectonics and geochemical composition of sandstones. *Jour. Geol.*, v.91, pp.611-627.
- [9] Bhatia, M.R. and Crook, K.A.W. (1986) Trace elements characteristics of greywackes and tectonic setting discrimination of sedimentary basins. *Contrib. Mineral. Petrol.*, v.92, pp.181-193.
- [10] Bhattacharya, H.N. and Mahapatra, S. (2007) Evolution of Proterozoic rift margin sediments, north Singhbhum mobile belt, Jharkhand-Orissa, India. *Precamb. Res.*, v.162, pp.302-316.
- [11] Bhushan, S.K. and Sahoo, P. (2010) Geochemistry of clastic sediments from Sargur Supracrustals and Bababudan Group, Karnataka: Implications on Archean-Proterozoic Boundary. *Jour. Geol. Soc. India*, v.75(6), pp.829-840.
- [12] Chakrabarti, K., Ecka, N.R.R., Mishra, B., Ramesh Babu, P.V. and Parihar, P.S. (2011) Paleoproterozoic Quartz-Pebble Conglomerate Type Uranium Mineralisation in Mankarhachua Area, Angul District, Orissa. *Jour. Geol. Soc. India*, v.77(5), pp.443-449.
- [13] Chakrabarti, K., Ecka, N.R.R., Mishra, B., Mahendra Kumar, K., Katti, V.J., Umamaheswar, K., Parihar, P.S., Mukhopadhyay, J. and Ghosh, G. (2013) Gold, silver and platinum group of elements mineralization in Precambrian uraniumiferous quartz-pebble conglomerates of Mankarhachua area, Angul District, Odisha. *Curr. Sci.*, v.105(7), pp.978-983.
- [14] Chaudhuri, T., Mazumder, R. and Arima, M. (2015) Petrography and geochemistry of Mesoarchean komatiites from the eastern Iron Ore belt, Singhbhum craton, India, and its similarity with 'Barberton type komatiite'. *Jour. Africa. Earth Sci.*, v.101, pp.135-147.
- [15] Chaudhuri, T., Satish, M., Mazumder, R. and Biswas, S. (2017) Geochemistry and Sm-Nd isotopic characteristics of the Paleoproterozoic Komatiites from Singhbhum Craton, Eastern India and their implications. *Precamb. Res.*, v.298, pp.385-402.

- [16] Condie, K.C. (1993) Chemical composition and evolution of the upper continental crust. Contrasting results from surface samples and shales. *Chem. Geol.*, v.104, pp.1-37.
- [17] Condie, K.C. (2006) Archean geodynamics: similar to or different from modern geodynamics? *Geophysical Monograph Series 164*. Washington, DC, American Geophysical Union, pp.47-59.
- [18] Condie, K.C. and Wronkiewicz, D.J. (1990) The Cr/Th ratio in Precambrian pelites from the Kaapvaal craton as an index of craton evolution. *Earth Planet Sci. Lett.*, v.97, pp.256-267.
- [19] Cox, R., Lowe, D.R. and Cullers, R.L. (1995) The influence of sediment recycling and basement composition on evolution of mudrock chemistry in the southwestern United States. *Geochim. Cosmochim. Acta*, v.59(14), pp.2919-2940.
- [20] Cullers, R.L. (1994) The controls on the major and trace element variation of shales, siltstone and sandstones of Pennsylvanian-Permian age from uplifted continental blocks in Colorado to platform sediment in Kansas, USA. *Geochim. Cosmochim. Acta*, v.58, pp.4955-4972.
- [21] Cullers, R.L. (2000) Geochemistry of the Mesoproterozoic Lakhandia shales in southeastern Yakutia, Russia: implications for mineralogical and provenance control, and recycling. *Precamb. Res.*, v.104(1), pp.77-93.
- [22] Cullers, R.L. and Graf, J. (1983) Rare earth elements in igneous rocks of the continental crust: intermediate and silicic rocks, ore petrogenesis. *In: Henderson, P. (Ed.), Rare earth Geochemistry*. Elsevier, Amsterdam, pp. 275-312.
- [23] Cuney, M. (2010) Evolution of Uranium Fractionation Processes through Time: Driving the Secular Variation of Uranium Deposit Types. *Econ. Geol.*, v.105(3), pp.553-569.
- [24] Dankert, B.T. and Hein, A.A.K. (2010) Evaluating the structural character and tectonic history of the Witwatersrand Basin. *Precamb. Res.*, v.177(1), pp.1-22.
- [25] Donaldson, J.A. and de Kemp, E.A. (1998) Archean quartz arenites in the Canadian shield: examples from the Superior and Churchill provinces. *Sedi. Geol.* v.120, pp.153-176.
- [26] Das, A.K., Awati, A.B. and Sahoo, P. (1988) Quartz-pebble conglomerates of the Singhbhum Craton, Bihar and Orissa. *Mem. Geol. Soc. India*, v.9, pp.83-87.
- [27] Dunn, J.A. (1940) Stratigraphy of south Singhbhum. *Mem. Geol. Surv. India*, v.63, pp.303-389.
- [28] Dunn, J.A. and Dey, A.K. (1942) The geology and petrology of Eastern Singhbhum and surrounding areas. *Mem. Geol. Surv. India*, v.69(2), pp.281-456.
- [29] Eriksson, K.A. (1978) Alluvial and destructive beach facies from the Archean Moodies Group, Barberton Mountain Land, South Africa and Swaziland. *Canada Soc. Petrol. Geol. Mem.*5, pp.287-311.
- [30] Fareduddin, J.A.S. (1990) Significance of occurrence of detrital pyrite and uraninite on the Kalasapura conglomerate, Karnataka. *Indian Minerals*, v.44, pp.335-340.
- [31] Feng, R. and Kerrich, R. (1990) Geochemistry of fine-grained clastic sediments in the Archean Abitibi greenstone belt, Canada: implications for provenance and tectonic setting. *Geochim. Cosmochim. Acta*, v.54, pp.1061-1081.
- [32] Fedo, C.M., Nesbitt, H.W. and Young, G.M. (1995) Unravelling the effects of potassium metasomatism in sedimentary rocks and paleosols with implications for paleoweathering conditions and provenance. *Geology*, v.23, pp.921-924.
- [33] Fedo, C.M. and Eriksson, K.A. (1996) Stratigraphic framework of the ~ 3 Ga Buhwa greenstone belt: a unique stable shelf succession in the Zimbabwe Archean craton. *Precamb. Res.*, v.77(3-4), pp.161-178.
- [34] Floyd, P.A., Winchester, J.A. and Park, R.G. (1989) Geochemistry and tectonic setting of Lewisian clastic metasediments from early Proterozoic Loch Maree Group of Gairloch, N.W, Scotland. *Precamb. Res.*, v.45(1-3), pp.203-214.
- [35] Frimmel, H.E. and Minter, W.E.L. (2002) Recent developments concerning the geological history and genesis of the Witwatersrand gold deposits, South Africa. *Soc. Eco. Geolo. Spec. Pub.*, no.9, pp.17-45.
- [36] Garde, A.A. (2007) A mid-Archean island arc complex in the eastern Akia terrane, Godthåbsfjord, southern West Greenland. *Jour. Geol. Soc. Lond.*, v.164, pp.565-579.
- [37] Ghosh, S., De, S. and Mukhopadhyay, J. (2016) Provenance of >2.8 Ga Keonjhar Quartzite, Singhbhum Craton, Eastern India: Implications for the Nature of Mesoarchean Upper Crust and Geodynamics. *Jour. Geol.*, v.124(3), pp.331-351.
- [38] Goswami, J.N., Misra, S., Wiedenbeck, M., Ray, S.L. and Saha, A.K. (1995)  $^{207}\text{Pb}/^{206}\text{Pb}$  ages from the OMG, the oldest recognized rock unit from Singhbhum-Orissa Iron Ore craton, E. India. *Curr. Sci.*, v.69(12), pp.1008-1012.
- [39] Grandstaff, D.E. (1980) Origin of uraniferous conglomerates at Elliot Lake, Canada and Witwatersrand, South Africa: implications for oxygen in the Precambrian Atmosphere. *Precamb. Res.*, v.13, pp.1-26.
- [40] Haque, M.W. and Dutta, S.K. (1996) Investigation for gold mineralization associated with shallow level acid-basic-ultrabasic rocks in Dhanjori basin along possible craton margin, East Singhbhum district, Bihar. *Rec. Geol. Surv. India*, v.129(3), pp.147-149.
- [41] Haque, M.W. and Dutta, S.K. (1999) Investigation for gold mineralization in the quartz-pebble conglomerates and associated rocks in the southern part of Dhanjori basin, East Singhbhum district, Bihar. *Rec. Geol. Surv. India*, v.131(3), pp.152-154.
- [42] Haque, M.W. and Dutta, S.K. (2001) Investigation for gold mineralization in the quartz-pebble conglomerates and associated rocks in the southern part of Dhanjori basin, East Singhbhum district, Bihar. *Rec. Geol. Surv. India*, v.132(3), pp.155-162.

- [43] Hamilton, W.B. (2013) Evolution of the Archean Mohorovičić discontinuity from a synaccretionary 4.5 Ga protocrust. *Tectonophysics*, v.609, pp.706-733.
- [44] Hayashi K., Fujisawa H., Holland H. and Ohmoto H. (1997) Geochemistry of ~1.9 Ga sedimentary rocks from northeastern Labrador. Canada, *Geochimica Cosmochimica Acta*, v.61(19), pp.4115-4137.
- [45] Hazen, R.M., Ewing, R.C. and Sverjensky, D.A. (2009) Evolution of uranium and thorium minerals. *Ameri. Min.*, v.94, pp.1293-1311.
- [46] Heron, M.M. (1988) Geochemical classification of terrigenous sands and shales from core and log data. *Jour. Sedi. Petrol.*, v.58(5), pp.820-829.
- [47] Holland, H.D. (1984) *The Chemical Evolution of the Atmosphere and the Oceans*. Princeton, New Jersey. John Wiley, New York. 598p.
- [48] Iyenger, S.V.P. and Murthy, Y.G.K., 1982: The evolution of the Archean Proterozoic crusts in parts of Bihar and Orissa, Eastern India. *Rec. Geol. Surv. India*, v.112, pp.1-5.
- [49] Jones, H.C. (1934) The iron ore deposits of Bihar and Orissa. *Mem. Geol. Surv. India*, v.63, 357p.
- [50] Kato, Y., Ohta, L., Tsunematsu, T., Watanabe, Y., Isozaki, Y., Maruyama, S. and Imai, N. (1998) Rare earth element variations in mid-Archean banded iron formations: implications for the chemistry of the ocean and continental and plate tectonics. *Geochim. Cosmochim. Acta*, v.62(21/22), pp.3475-3497.
- [51] Kumar, A., Birua, S.N.S., Pande, D., Nath, A.R., Ramesh Babu, P.V. and Pandit, S.A. (2009) Radioactive quartz-pebble conglomerates from western margin of Bonai Granite pluton, Sundargarh district, Orissa – a new find. *Jour. Geol. Soc. India*, v.73(4), pp.537-542.
- [52] Kumar, A., Mishra, B., Chakrabarti, K., Ecka, N.R.R., Ramesh Babu, P.V. and Parihar, P.S. (2011a) Petrographic and geochemical characterization of quartz-pebble conglomerates from Koira and Daitari basins of Orissa. *Indian Mineralogist*, Min. Soc. India, Mysore, Golden Jubilee, v.45(1), pp.9-23.
- [53] Kumar, A., Venkatesh, A.S., Ramesh Babu, P.V. and Nandakishore, S. (2011b) A Note on the presence of Au-REE ± Ag-Pt in uraniferous Archean Iron Ore Group sediments, Western margin of Bonai Granite pluton, Eastern India. *Jour. Explor. Res. Atom. Min.*, (EARFAM), AMD, DAE, Hyderabad, v.21, pp.9-21.
- [54] Kumar, A., Venkatesh, A.S., Ramesh Babu, P.V. and Nayak, S. (2012) Genetic implications of Rare Uraninite and Pyrite in Quartz-Pebble Conglomerates from Sundargarh District of Orissa, Eastern India. *Jour. Geol. Soc. India*, v.79(3), pp.279-286.
- [55] Kumar, A., Venkatesh, A.S., Kumar, P., Rai, A.K. and Parihar, P.S. (2017) Geochemistry of Archean Radioactive Quartz Pebble Conglomerates and Quartzites from western margin of Singhbhum-Orissa Craton, eastern India: Implications on Paleoweathering, provenance and tectonic setting. *Ore Geol. Rev.* v.89, pp.390-406.
- [56] Krauskopf, K. (1967) *Introduction to Geochemistry*, Stanford University, Stanford. Mc Graw-Hill Book Co., New York, 721p.
- [57] Kroonenberg, S.B. (1994) Effects of provenance, sorting and weathering on the geochemistry of fluvial sands from different tectonic and climatic environments: Proceedings of the 29<sup>th</sup> Inter. Geol. Cong., Part A, pp.69-81.
- [58] Lowe, D.R. (1994) Archean greenstone-related sedimentary rocks. *In: Condie, K. C., ed. Archean crustal evolution*. Amsterdam, Elsevier, pp.121-170.
- [59] Mahadevan, T.M. (1986) Space-time controls in Precambrian uranium mineralisation in India. *Jour. Geol. Soc. India*, v.27(1), pp.47-62.
- [60] McLennan, S.M. (1989) Rare earth elements in sedimentary rocks- Influence of provenance and sedimentary processes. *Rev. Min.*, v.21, pp.169-200.
- [61] McLennan, S.M. and Taylor, S.R. (1991) Sedimentary rocks and crustal evolution: Tectonic setting and secular trends. *Jour. Geol.*, v.99, pp.1-21.
- [62] McLennan, S.M. (2001) Relationships between the trace element composition of sedimentary rocks and upper continental crust. *Geochem. Geophys. Geosyst.*, v.2(4), pp.1021-1024.
- [63] McLennan, S.M. and Taylor, S.R. (1991) Sedimentary rocks and crustal evolution: Tectonic setting and secular trends. *Jour. Geol.*, v.99, pp.1-21.
- [64] McLennan, S.M., Hemming, S., McDaniel, D.K. and Hanson, G.N. (1993) Geochemical approaches to sedimentation, provenance and tectonics. *In: Processes controlling the composition of clastic sediments* (Johnsson, M. J. and Basu, A, edited). *Geol. Soc. Amer. Spec. paper*, v.284, pp.21-40.
- [65] Mikhailov, V.A. (2006) Composition and genesis of Precambrian metalliferous conglomerates. *Litho. Min. Res.*, v.41(4), pp.389-398.
- [66] Misra, S. (2006) Precambrian chronostratigraphic growth of Singhbhum-Orissa Craton, eastern Indian Shield: an alternative model. *Jour. Geol. Soc. India*, v.67(3), pp.356-378.
- [67] Mishra, K.S., Durairaju, S., Rajasekharan, P. and Das, A.K. (1997) Occurrence of U-Au-REE bearing quartz-pebble conglomerate at Sayamba-Taldih, Sundargarh district, Orissa. *Jour. Geol. Soc. India*, v.50, pp.93-94.
- [68] Mishra, S., Deomurari, M.P., Wiedenbeck, M., Goswami, J.N., Ray, S.L. and Saha, A.K. (1999) <sup>207</sup>Pb/<sup>206</sup>Pb zircon ages and the evolution of Singhbhum craton, eastern India: an ion microprobe study. *Precamb. Res.*, v.93, pp.139-151.
- [69] Mishra, B., Pande, D., Gogoi, J., Kumar, A., Ramesh Babu, P.V. and Parihar, P.S. (2008) Quartz-Pebble Conglomerate Type Uranium Mineralization in Balia-Rankia Area of Daitari-Tomka basin, Jaipur district, Orissa. *Jour. Explor. Res. Atoms. Min.*, v.18, pp.1-14.
- [70] Mossman, D.J. and Harron, G.A. (1983) Witwatersrand-Type Paleoplacer Gold in the Huronian Supergroup of Ontario, Canada. *Geosci. Canada*, v.11(1), pp.33-40.

- [71] Mowbray, T.De. and Visser, M.J. (1984) Reactivation surfaces in subtidal channel deposits, Oosterschelde, southwest Netherlands. *Jour. Sedi. Petro.*, v.54, pp.811-824.
- [72] Mukhopadhyay, D. (2001) The Archean nucleus of Singhbhum: the present state of knowledge. *Gond. Res.*, v.4(3), pp.307-318.
- [73] Mukhopadhyay, J., Beukes, N.J., Armstrong, R.A., Zimmermann, U., Ghosh, G. and Medda, R.A. (2008) Dating the oldest greenstone in India: A 3.51 Ga precise U-Pb SHRIMP zircon age for dacitic lava of the Southern Iron Ore Group, Singhbhum Craton. *Jour. Geol.*, v.116(5), pp.449-461.
- [74] Mukhopadhyay, J., Ghosh, G., Zimmermann, U., Guha, S. and Mukherjee, T. (2012) A 3.51Ga bimodal volcanics-BIF-ultramafic succession from Singhbhum craton: implications for Palaeoarchean geodynamic processes from the oldest greenstone succession of the Indian subcontinent. *Geol. Jour.*, v.47, pp.284-311.
- [75] Mukhopadhyay, J., Crowley, Q.G., Ghosh, S., Ghosh, G., Chakrabarti, K., Misra, B., Heron, K. and Bose, S. (2014) Oxygenation of the Archean atmosphere: New paleosol constraints from eastern India: *Geology*, v.43, pp.923-926.
- [76] Mukhopadhyay, J., Mishra, B., Chakrabarti, K., Ghosh, G. and De, S. (2016) Uraniferous Paleoplacers of the Mesoarchean Mahagiri Quartzite, Singhbhum Craton, India: Depositional Controls, Nature and Source of >3.0Ga Detrital Uraninites. *Ore Geol.*, v.72, pp.1290-1306.
- [77] Murthy, V.N. and Acharya, S. (1975) Lithostratigraphy of the Precambrian rocks around Koira, Sundergarh district, Orissa. *Jour. Geol. Soc. India*, v.16, pp.55-68.
- [78] Naqvi, S.M., Narayana, B.L., Rama Rao, R., Ahmad, S.M. and Udai Raj, B. (1980) Geology and geochemistry of the paragneisses from Jawanahalli schist belt, Karnataka, India. *Jour. Geol. Soc. India*, v.21, pp.577-592.
- [79] Nesbitt, H.W. and Young, G.M. (1982) Early Proterozoic climates and plate motions inferred from major element chemistry of lutites. *Nature*, v.299, pp.715-717.
- [80] Nesbitt, H.W. and Young, G.M. (1984) Prediction of some weathering trends of plutonic and volcanic rocks based on thermodynamic and kinetic considerations. *Geochim. Cosmochim. Acta*, v.48(7), pp.1523-1534.
- [81] Nesbitt, H.W., McLennan, S.M. and Keays, R.R. (1996) Effects of chemical weathering and sorting on the petrogenesis of siliciclastic sediments with implications for provenance studies. *Jour. Geol.*, v.104(5), pp.525-542.
- [82] Pandit, S.A. (2002) Uranium occurrences in the quartz-pebble conglomerate in Karnataka. *EARFAM, AMD, Hyderabad*, v.14, pp.131-146.
- [83] Phillips, G.N. and Law, J.D.M. (2000) Witwatersrand gold fields: geology, genesis and exploration. *Soc. Econ. Geol.*, v.13, pp.439-500.
- [84] Pettijohn, F.J., Potter, P.E. and Siever, R. (1972) *Sand and Sandstones*. Springer-verlag, New York, 619p.
- [85] Rama Rao, B.V. (1974) Discovery of uraniferous Precambrian conglomerates at Chikmagalur, Karnataka state. *Curr. Sci.*, v.44, pp.174-175.
- [86] Rajanikanta, M.S., Manikyamba, C., Ganguly, S., Ray, J., Santosh, M., Dhanakumar, Th.S. and Chandan Kumar, B. (2017) Paleoproterozoic arc basalt-boninite-high magnesian andesite-Nb enriched basalt association from the Malangtoli volcanic suite, Singhbhum Craton, eastern India: Geochemical record for subduction initiation to arc maturation continuum. *Jour. Asian Earth Sci.*, v.134, pp.191-206.
- [87] Robertson, D.S. (1962) Thorium and uranium in Blind River ores. *Econ. Geol.*, v.57, pp.1175-1184.
- [88] Robinson, A. and Spooner, E.T.C. (1982) Source of the detrital components of uraniferous conglomerates, Quirke ore zone, Elliot Lake, Ontario, Canada. *Nature*, v.299, pp.622-624.
- [89] Ronald, E.S. (2015) Uraniferous Conglomerates: thoughts on their origins. *Segate News Letter*, no.103, pp.8-10.
- [90] Roscoe, S.M. (1973) The Huronian Supergroup, a Paleoproterozoic succession showing evidence of atmospheric evolution. *Geol. Associ. Canada, Spec. Paper no.12*, pp.31-47.
- [91] Roser, B.P. and Korsch, R.J. (1986) Determination of tectonic setting of sandstone mudstone suites using SiO<sub>2</sub> content and K<sub>2</sub>O/Na<sub>2</sub>O ratio. *Jour. Geol.*, v.94, pp.635-650.
- [92] Roser, B.P. and Korsch, R.J. (1988) Provenance signatures of sandstone- mudstone suites determined using discriminant functions analysis of major element data. *Chem. Geol.*, v.67, pp.119-139.
- [93] Saager, R. and Stupp, H.D. (1983) U-Ti phases from Precambrian Quartz-pebble conglomerates of the Elliot Lake area, Canada and the Pongoloa Basin, South Africa. *TMPM Tschermaks Min. Petr. Mitt, Federal Repub. German*, v.32, pp.83-102.
- [94] Saha, A.K. (1994) Crustal evolution of Singhbhum-North Orissa, eastern India. *Mem. Geol. Soc. India*, v.27, 341p.
- [95] Sahu, N.K., Swain, P.K., Mohanty, S.N. and Mukherjee, M.M. (1998) Marginal basin arc basalts of Nuakot volcanics, Keonjhar district, Odisha: a petrochemical appraisal. (Abs.) *Inter. Semi. Precamb. crust of Eastern and Central India, (UNESCO-IUGS-IGCP-368)*, Bhubaneswar, pp.103-108.
- [96] Sarangi, S.K. and Acharya, S. (1975) Stratigraphy of the Iron Ore Group around Khandadhar, Sundargarh district, Orissa. *Indian Jour. Earth Sci.*, v.2(2), pp.182-189.
- [97] Scarpelli, W. (1991) Precambrian auriferous quartz-pebble conglomerates in Brazil. In: Hérail Gérard (ed.), Fornari Michel (ed.). *Gisements alluviaux d'or = Alluvial gold placers = Yacimientos aluviales de oro. La Paz: ORSTOM*, 261-273. (Colloques et Séminaires). *Symp. Intern., sur les Gisements Alluviaux d'Or, La Paz (BOL)*, 1991/06/03-05. ISSN 0767-2896.
- [98] Schidlowski, M. (1975) Uraniferous constituents of the Witwatersrand conglomerates: Ore microscopic

- observations and implications for the Witwatersrand metallogeny. *In: genesis of uranium and gold bearing Precambrian quartz-pebble conglomerates*, USGS Prof. Paper, 1161-A-BB, N1-N24.
- [99] Smith, N.D. and Minter, W.E.L. (1980) Sedimentological controls of gold and uranium in two Witwatersrand palaeo-placers. *Econ. Geol.*, v.75(1), pp.1-14.
- [100] Smithies, R. H., Champion, D., van Kranendonk, M., Howard, H. and Hickman, A. (2005) Modern-style subduction processes in the Mesoarchean: geochemical evidence from the 3.12 Ga Whundo intra-oceanic arc. *Earth Planet. Sci. Lett.*, v.231(3-4), pp.221-237.
- [101] Srinivasan, G. and Ojakangas, R.W. (1986) Sedimentology of quartz-pebble conglomerates and quartzites of the Archean Bababudan Group, Dharwar craton, South India: evidence for early crustal stability. *Jour. Geol.*, v.94(2), pp.199-214.
- [102] Sunilkumar, T.S., Parthasarathi, R., Palrecha, M.M., Shah, V.L., Sinha, K.K. and Krishna Rao, N. (1996) Chemical age of detrital zircons from basal quartz-pebble conglomerates of Dhanjori Group, Singhbhum Craton, eastern India. *Curr. Sci.*, v.71(6), pp.482-486.
- [103] Sunilkumar, T.S., Krishna Rao, N., Palrecha, M.M., Parthasarathi, R., Shah, V.L. and Sinha, K.K. (1998) Mineralogical and geochemical characteristic of basal quartz-pebble conglomerates of Dhanjori Group, Singhbhum Craton, India and their significance. *Jour. Geol. Soc. India*, v.51(6), pp.761-776.
- [104] Suttner, L.J. and Dutta, P.K. (1986) Alluvial sandstone composition and paleoclimate, I. Framework mineralogy. *Jour. Sedim. Petrol.*, v.56, pp.329-345.
- [105] Taylor, S.R. and McLennan, S.M. (1985) *The continental Crust: Its composition and evolution*. Blackwell. Blackwell Scientific, Oxford, 311p.
- [106] Taylor, S. R. and McLennan, S. M. (2009) *Planetary crusts: their composition, origin and evolution*. Cambridge, Cambridge University Press, 378 p.
- [107] Theis, N.J. (1979) Uranium-bearing and associated minerals in their geochemical and sedimentological context, Elliot Lake, Ontario. *Geol. Surv. Canada Bull.*, v.304, 50p.
- [108] Uvarova, Y.A., Kyser, T.K., Geagea, M.L. and Chipley, D. (2014) Variations in the uranium isotopic compositions of uranium ores from different types of uranium deposits. *Geochim. Cosmochim. Acta*, v.146, pp.1-17.
- [109] Vasudeva Rao, M., Sinha, K.K., Mishra, B., Balachandran, K., Srinivasan, S. and Rajasekharan, P. (1988) Quartz-pebble conglomerate from the Dhanjori-Singhbhum uranium Province. *Mem. Geol. Soc. India*, v.9, pp.89-95.
- [110] Vearncombe, S. and Kerrich, R. (1999) Geochemistry and geodynamic setting of volcanic and plutonic rocks associated with early Archaean volcanogenic massive sulphide mineralization, Pilbara craton. *Precamb. Res.*, v.98, pp.243-270.
- [111] Viswanath, R.V., Roy, M.K., Pandit, S.A. and Narayan Das, G.R. (1988) Uranium mineralization in the Quartz- Pebble Conglomerates of Dharwar Supergroup, Karnataka. *Mem. Geol. Soc. India*, v.9, pp.33-41.
- [112] Wronkiewicz, D.J. and Condie, K.C. (1987) Geochemistry of Archean shales from the Witwatersrand supergroup, South Africa: source area weathering and provenance. *Geochim. Cosmochim. Acta*, v.54, pp.2401-2416.
- [113] Wronkiewicz, D.J. and Condie, K.C. (1989) Geochemistry and provenance of sediments from the Pongola Supergroup, South Africa: Evidence for a 3.0 Ga old continental craton. *Geochim. Cosmochim. Acta*, v.53(7), pp.1537-1549.
- [114] Yadav, P.K. and Ghosh, A. (2013) Specialised Thematic Mapping around Kudarsahi-Kuchaiburi-Kuhisila area, Badampahar-Gorumahisani Belt, Mayurbhanj District, Odisha with special emphasis on search for gold mineralization. *Unpub. Rep. Geol. Surv. India, F.S. 2012-13*.
- [115] Yadav, P.K., Pradhan, U.K., Mukherjee, A., Sar, R.N., Sahoo, P. and Das, M. (2015) Basic characterization of Kapili Komatiite from Badampahar-Gorumahisani Schist Belt, Singhbhum Craton, Odisha, India. *Indian Jour. Geosci.*, v.69(1), pp.1-12.
- [116] Yadav, P.K., Sahoo, P., Pradhan, U.K. and Das, M. (2016) Komatiite from Mesoarchean Badampahar-Gorumahisani greenstone belt, Singhbhum craton, eastern India: Petrogenetic affinity with 'Barberton type'. 35<sup>th</sup> Inter. Geosci. Cong., Paper No. 671, Cape Town, South Africa.
- [117] Yadav, P.K., Chaudhuri, T. and Das, A. (2016) Specialised Thematic Mapping in the transect between Luhakorha and Karanjia in the central part of Singhbhum Craton, Kendujhar district, Odisha. *Unpub. Rep. Geol. Surv. India, F.S. 2014-16*.
- [118] Yadav, P.K. (2017) Incidence of uranium and thorium mineralization in quartz-pebble conglomerate of Koira Group, Singhbhum Craton, India. *Inter. Jour. Res. Anal. Rev.*, v.4(4), pp.484-488.
- [119] Yadav, P.K. and Das, M. (2017) Petrology, geochemistry and petrogenesis of Al-depleted komatiite from Badampahar-Gorumahisani Greenstone Belt of Eastern Iron Ore Group, Singhbhum Craton, India. *Indian Jour. Geosci.*, v.70(3&4) & 71(1), pp.313-328.
- [120] Yadav, P.K. and Das, M. (2017) Geochemistry of Kapili Komatiite from Badampahar-Gorumahisani greenstone belt, Singhbhum craton, India and its resemblance with 'Barberton Komatiite'. *Inter. Jour. Res. Anal. Rev.*, v.4(4), pp.495-507.
- [121] Yadav, P.K. and Das, M. (2018) Gold, uranium and thorium mineralization in Paleoproterozoic quartz-pebble conglomerate of Dhanjori Group, Singhbhum Craton, India. *Indian Jour. Geosci.*, v.72(2), pp.139-150.
- [122] Yadav, P.K. and Das, M. (2019) Geochemistry of Mesoarchean felsic tuff from Bonai-Kendujhar belt of Western Iron Ore Group, Singhbhum Craton, India: implications for volcanic arc tectonic setting. *Indian Jour. Geosci.*, v.73(1), pp.1-14.

- [123] Yadav, P.K. and Das, M. (2019) Anomalous high values of rare earth element in quartz-pebble conglomerate of Koira Group of Western Iron Ore Group, Singhbhum Craton, India. *Indian Jour. Geosci.*, v.73(2), pp.131-142.
- [124] Yadav, P.K., Das, M. and Ray, S. (2020) Petrochemical signatures of meta-andesite from Badampahar-Gorumahisani Greenstone Belt, Singhbhum Craton: Implication on Precambrian tectonic setting of the Eastern India Shield. Accepted manuscript for the *Indian Jour. Geosci.*, v.74(1), pp.33-55.
- [125] Yang, W. and Holland, H.D. (2002) The redox-sensitive trace elements, Mo, U and Re in Precambrian carbonaceous shales: Indicators of the Great Oxidation Event (abs.). *Geol. Soc. America, Abst and Progrm.*, v.34, pp.381.